ALEPH 91-43
MINIV 91-002
D. Brown et al.
25.3.1991

Alignment of the ALEPH Silicon Vertex Detector

David Brown, Jochen Lauber, Lorenzo Moneta,Roberto Dell'Orso, George Redlinger, Cristina Vannini, Andrew Weir

Abstract

A program for aligning the VDET using ITC-TPC tracks has been developed. This uses techniques which avoid the systematic accuracy limits of the TPC and ITC. Using this program, alignment constants for the 1990 run have been produced, with errors of $\sim 6 \oplus 7\mu$ (statistical plus systematic) in the $R-\phi$ direction, $\sim 15 \oplus 15\mu$ in the Z. This same program will function for 1991 data.

Thus, the degrees of freedom represented by the global alignment are completely *redundant* with the local alignment. The only real function of the global alignment is therefore to ensure that the local alignment corrections are kept small, so that the (linearized) correction routines used in the local alignment are not extended beyond their proper limits ($\sim 1mm$).

1.2 Local VDET Alignment

A natural system for the VDET alignment is to have for each wafer 6 constants, representing the 6 degrees of freedom available to a rigid object in 3-space. These 6 degrees of freedom break down into 3 translations and 3 rotations. By convention, these are expressed in the nominal *wafer local* coordinate system, with axes labeled VUW. This coordinate system is referred to throughout this note. V points perpendicular to the wafer surface outwards from the interaction point, U lies in the wafer plane, and points in the $+\phi$ direction, while W points along the $+Z$ axis. VUW is a right-handed system. The alignment is then defined as a small vector displacement $\vec{V_0}$ of the wafer center from its nominal position, plus a small (right-handed) rotation $\vec{\alpha}$ about each of the axes. In the alignment procedure, the best alignment for each wafer is found in the 6-dimensional $\vec{V_0} \times \vec{\alpha}$ space, and a full error correlation matrix is computed.

When the statistical error on the alignment is propagated to an error on a VDET hit, we observe that this error is not uniform across the wafer. Consider for example an alignment generated by measuring a set of points on a wafer, with these points distributed evenly across the wafer, all having equal errors. These points can come from tracks or microscope measurements or anything else. Then consider two VDET hits, one at the wafer center, the other at the wafer edge in the W direction. The statistical error on the U coordinate for the hit at the W edge is *twice* that of the U coordinate at the wafer center. In fact, the U error depends quadratically on the W displacement, having a minimum at the wafer center. This is demonstrated graphically in figure 2, which plots the U error as a function of W, relative to the error on the translational term δ_{U_0}. This effect comes solely from allowing the angular degree of freedom in the alignment parameterization, independent of the choice of rotation point. Because of this non-uniformity, henceforward we will discuss measurements and calculations for alignment errors *averaged* over the wafer surface. In the simple model discussed above, this average is $\sim 1.4\times$ the translation term error.

2 Alignment Precision

Before starting to develop alignment techniques, it was necessary to understand the precision required. The alignment precision is in turn determined by the physics requirements, and the intrinsic limitations of the device. Most VDET physics involves using the *impact parameter* of tracks fit through the VDET. Given this, and the intrinsic point resolution of the VDET (measured in testbeam studies), one can determine alignment precision requirements.

We adopt a standard whereby the alignment uncertainty does not significantly degrade the impact parameter resolution which can be measured with dimuon data. More precisely, our standard allows a 10parameter resolution due to misalignment for the 1990 VDET and a 5increase for the 1991 VDET. The difference in the tolerances reflects the expected improvement in the number of dimuon events in the data.

2.1 VDET point resolution

The VDET point resolution was measured in the 1988 November testbeam. The results are described in two theses (by Christian Bauer and Lorenzo Moneta). These results give a resolution in the U direction of 12 μ , and in the W of 16 μ for normal incidence tracks, with no magnetic field, and a signal:noise of $\sim$ 11:1 (13:1) on the U (W) side. While the effect of the magnetic field is unknown, it is easy to estimate the effect of non-normal track angles. We construct a simple model which assumes that the charge deposited by a track is proportional to the path length in the silicon, and is evenly collected by all strips it passes. From this assumption, the strip pitch (readout and floating), and the signal:noise, one can predict the resolution as;

$$\sigma_{res}^2 = \left(\frac{\mathcal{P}_f \cos\theta_\perp}{\sqrt{12}}\right)^2 + \left(\frac{\mathcal{P}_r}{\mathcal{S}:\mathcal{N}} \frac{1+\mathcal{S}_s \sin\theta_\perp}{\sqrt{1+\sin^2\theta_\perp + \sin^2\theta_{||}}}\right)^2$$

where

$$\begin{aligned}
\theta_\perp &= \text{Angle across the strips} \\
\theta_{||} &= \text{Angle along the strips} \\
\mathcal{S}_s &= \text{Shower spread factor} \approx \frac{3}{2} \\
\mathcal{P}_r &= \text{Readout strip pitch} = 100\ \mu\ U \text{ and } W \\
\mathcal{P}_f &= \text{Floating strip pitch} = 25\ (50)\ \mu\ U\ (W)
\end{aligned}$$

The first term in the equation represents the physical limit to the resolution given by the floating strip pitch, while the second represents the resolution degradation given by the noise. Given the $\mathcal{S}:\mathcal{N}$ values listed above, this formula predicts a U (W) resolution for normal incident tracks of 11.6 (16.4) μ, in good agreement with the measured values. Figure 3 plots the predicted variation in resolution over the range of angles possible for tracks hitting the VDET. The variation is small, and for the purposes of this analysis, we take a constant resolution of 13 (16) μ in the U (W) direction.

2.2 Impact Parameter Resolution

The impact parameter resolution was studied with a simple extension of the existing (i.e. no VDET) Monte Carlo. We used high momentum tracks from tau events to set the standard for the alignment error we can tolerate; this is of course the most stringent standard since most physics

Table 1: Tracking resolution for MC tracks with $p_t > 20$ GeV

	$\sigma_{p_t}/p_t^2\,(GeV^{-1} \times 10^{-4})$	$\sigma_{\tan\lambda}(\times 10^{-4})$	$\sigma_{\phi_0}(mrad)$	$\sigma_{D_0}(\mu m)$	$\sigma_{Z_0}(\mu m)$
TPC+ITC only	10.5 ± 0.1	6.71 ± 0.09	0.41 ± 0.05	113 ± 1	750 ± 11
+VDET '90					
Inner layer only	8.0 ± 0.1	2.67 ± 0.03	0.27 ± 0.03	30.1 ± 0.3	31.2 ± 0.4
Two layers	8.0 ± 0.1	2.59 ± 0.04	0.27 ± 0.05	29.8 ± 0.5	29.3 ± 0.4
+VDET '91					
Inner layer only	7.5 ± 0.1	2.59 ± 0.03	0.25 ± 0.03	22.1 ± 0.2	23.7 ± 0.3
Two layers	7.1 ± 0.1	2.30 ± 0.03	0.23 ± 0.03	21.7 ± 0.3	23.0 ± 0.2

analyses will be concerned with lower momentum tracks where multiple scattering will reduce the relative contribution of alignment errors.

Our event sample consisted of a set of KORALZ tau events processed through Galeph 239 and Julia 241. Only tracks with p_t greater than 20 GeV were used in this study. These tracks were then given VDET hits by taking the Monte Carlo "truth" information for the track parameters, propagating the track to the VDET wafers (including the proper geometry), and then smearing the position with a Gaussian with sigma $13\mu m$ in $R - \phi$ and $16\mu m$ in Z. The muons were then refit and the reconstructed track parameters compared to the "truth" information. The results are shown in table 1.

2.3 VDET precision

To propagate the requirement on impact parameter resolution onto requirements for VDET precision, we must understand how a VDET misalignment affects the impact parameter. To understand this connection, we consider a simple model of ALEPH tracking including VDET which assumes that the high statistical precision will force the tracks through the VDET points.

We consider the 1990 and 1991 versions of the VDET separately, both through their geometry, and their *efficiency*. For the 1990 VDET, the single-hit efficiency was $\sim 30\%$, making the probability of a track generating a hit in both layers small. Consequently, we assume for 1990 that each track has only a single VDET hit and that all the angular information comes from the outer tracking detectors. Conversely, it is hoped that the 1991 VDET will have a much higher efficiency, and so we assume for 1991 that all tracks go through both VDET layers.

Figure 4 demonstrates how the impact parameter changes for various misalignments when a track goes through 2 layers. Taking the VDET wafer as a rigid object, the misalignments break down into 4 categories; planar translations, planar rotations, radial translation, and out-of-plane rotations. These have decreasing effect on the impact parameter, but all show a basic linear relation between misalignment and impact parameter. For tracks going through a single VDET layer, the correlation between misalignments and impact parameter resolution is direct; planar displacements and rotations have a unitary effect, while radial displacements and out-of-plane rotations have a second-order effect.

Table 2 lists the average values of the these linear factors, for the 1990 geometry, assuming a uniform track illumination of all the VDET wafer surfaces. The numbers in the table describe how the misalignments affect the impact parameter in the $R - \phi$ and Z directions.

Using the information in table 2 and impact parameter resolutions from table 1 (i.e. $30\mu m$ in $R - \phi$ and $31\mu m$ in Z for the 1990 VDET), we determine the alignment requirements as follows. Taking a limit of 10% worsening of impact parameter, the 1 σ limits on alignment parameter X is

Table 2: Average impact parameter factors for the 1990 geometry

	$\langle\frac{\Delta I}{\Delta V}\rangle$	$\langle\frac{\Delta I}{\Delta U}\rangle$	$\langle\frac{\Delta I}{\Delta W}\rangle$	$\langle\frac{\Delta I}{\alpha_V}\rangle$	$\langle\frac{\Delta I}{\alpha_U}\rangle = \langle\frac{\Delta I}{\alpha_W}\rangle$
In $R-\phi$	0.1	1.0	0.0	15 μ/mrad	2.6 μ/mrad
In Z	0.4	0.0	1.0	13 μ/mrad	7 μ/mrad

Table 3: 1 σ tolerances on VDET alignment parameters

Year	$\Delta V(\mu m)$	$\Delta U(\mu m)$	$\Delta W(\mu m)$	$\alpha_V(mrad)$	$\alpha_U = \alpha_W(mrad)$
1990 testbeam resolution	36	14	14	0.9	2.0
1990 ALEPH resolution	61	20	24	1.3	3.5
1991 testbeam resolution	15	7	7	0.5	0.8

given by the simple formula;

$$\Delta X_{1\sigma} \equiv \frac{\Delta I_{1\sigma} \times \sqrt{1.1^2 - 1}}{\langle\frac{\Delta I}{\Delta X}\rangle}$$

These values are listed in table 3. In each case, we examined the effect of the different misalignments on both the $R-\phi$ and Z impact parameter, and chose the more stringent requirement.

For the 1991 VDET (where we assume two hits per track), the TPC-ITC system has an angular resolution comparable to that of the VDET, so that we cannot assume that the track will be forced to pass exactly through both VDET hits. For example, if a single VDET layer is misaligned, the track fit could prefer to maintain the track angle rather than forcing the track to pass through both hits, thus changing the angle. Therefore, we use a different model to determine the alignment tolerances.

To obtain the tolerances, we use the Monte Carlo described in the previous section, but *smear* the positions of the VDET hits to account for alignment effects, before refitting the track. The results are shown in Figure 5. We take as an example the V displacement of $20\mu m$ to describe how the points in these plots are derived. Each event, the position of each wafer is smeared in V by a Gaussian of width $20\mu m$, in addition to the VDET point resolution. The track is then refit with the VDET hits. The impact parameter resolution is then calculated as the width of the distribution comparing the reconstructed impact parameter with the Monte Carlo "truth" value. This impact parameter resolution is then divided by the resolution with no smearing for alignment effects.

The figures show that the impact parameter resolution in Z is more sensitive than that in $R-\phi$ for four of the six alignment parameters: V, W, α_U, and α_W. The effect of the planar rotation, α_V, is almost the same in both dimensions. The Z sensitivity is also evident in the analytical calculation results summarized in Table 2. This is because the tracks cross the VDET wafers closer to normal incidence in the $R-\phi$ plane than in the $R-Z$ plane.

Taking a limit of 5% degradation of the impact parameter resolution to set the tolerance, the values for the 1991 VDET are shown in Table 3.

3 Alignment Methods

The basic idea used in the VDET alignment is to position the wafer so as to minimize the discrepancy between the VDET hits and the position of the TPC-ITC tracks (extrapolated to the VDET). The weakness of this method is that any systematic errors present in the TPC or ITC will be transferred directly to the VDET. If this situation were left untreated, tracks refit using the VDET would have a smaller statistical error on their impact parameters, but would have a *systematic error* equal to that seen in the TPC-ITC. Thus, if the VDET were aligned simply by positioning the wafers where they agree best with the ITC-TPC, the resultant impact parameter resolution (statistical and systematic combined) would not improve.

To avoid this situation, we must effectively reduce the systematic errors on the ITC-TPC tracks. Given that these systems have been internally aligned to the statistical limit of the available data (see ALEPH note 90-156 TPCGEN 90-8), any improvement must come from outside. We have developed methods (overlap, 2-layer, and muon pair) which use the information from the VDET itself to *bootstrap* the detector into alignment. The overlap and 2-layer techniques provide directly the relative position of nearby wafers, virtually free from systematic errors, but only indirectly the relative positions of distant wafers. The muon pair technique is sensitive to the position of wafers on opposite sides of the detector (in Z and ϕ).

By contrast, we also have a procedure (vertex constraint) which improves on the tracks by requiring a global consistency to the events, without using VDET information. This reduces the systematic errors, but does not completely eliminate them. By contrast with methods using VDET data, this procedure gives wafer positions relative to the ITC-TPC.

The idea embodied in the VDET local alignment is to apply all 4 techniques simultaneously, solving for the wafer positions by requiring a consistency between and within the methods. The final result should then express the best features of each; accurate relative wafer positions from the VDET data constrained procedures, and accurate positions relative to the ITC-TPC from the combination of the global constraint techniques with the global consistency of the VDET data constraints.

3.1 Vertex Constraint Method

The basic idea of a vertex constraint is to refit the tracks in an event including for each a new point which corresponds to the single vertex from where they originate. This point can be estimated using the tracks themselves. By including this point, one reduces both the statistical and systematic errors on the track parameters. The systematic error is reduced because the new point effectively *averages* local misalignments of the TPC-ITC.

Using tracks with a vertex constraint refit necessitates rejecting tracks which do not come from the primary event vertex. Once such tracks have been eliminated, the remaining tracks can be combined to estimate the primary event vertex, and it is then assumed that these tracks all originated at the primary event vertex. In this section we describe the track selection criteria, and the algorithm used to determine the primary event vertex. The track cuts and vertex finding are within the subroutine EVTVTX which calls V0CHUK to flag tracks from detached vertices.

3.1.1 Track selection criteria

The tracks which are used to estimate the position of the primary event vertex (and subsequently used to align the VDET) must satisfy the following cuts :-

- momentum > 1.5 GeV/c.
- more than 3 ITC hits and more than 7 TPC hits.
- χ^2 per degree of freedom less than 5.0.

- D_0, the distance of closest approach in the $R-\phi$ plane to the nominal beam position, less than $1250\mu m$.
- the Z position at D_0 closer than $5cm$ to the detector origin.
- tracks were required to be inconsistent with coming from an identified detached vertex.

There are, on average, 6.2 such tracks in a QCD event. Events which contained less than two tracks passing these cuts were rejected. Clearly, it is impossible to reject secondary tracks with 100% efficiency while retaining only primary tracks, but these cuts were a reasonable tradeoff between efficiency and accuracy in determining the primary event vertex.

3.1.2 Vertex finding algorithm

The primary vertex finding algorithm was designed to be fast and reasonably accurate. An assumption which made the algorithm fast was that the tracks could be well approximated near the origin by straight lines (the curvature of tracks with momentum greater than 1.5 GeV/c is very small over small distance scales). Thus a given track could be described in the $R-\phi$ plane by a point lying on the track, and the phi angle of the track at that point. The algorithm also uses the beam position, estimated by using all tracks averaged over a fill (the variables QVXNOM and QVYNOM in ALPHA). In future the Beam Orbit Monitors (BOMs) may provide a more accurate estimate of the beam position on an event by event basis.

The first step in the algorithm was to estimate the thrust axis for the selected tracks using the standard ALEPH routine QJTHRU. This thrust axis was then required to pass through the beam position point (QVXNOM,QVYNOM) in the x,y plane (line **T** in figure 6A). The normal to this thrust axis was calculated (line N in figure 6A), and also required to pass through the beam position point. The estimated primary event vertex in the x,y plane was then simply the weighted mean position of where the selected tracks crossed this normal direction. The weight given to each track was the cosine of the angle at which the track crossed the line **N**, divided by the estimate of the error on the track's distance of closest approach to the origin (taken from the FRFT bank).

In order to find the Z position of the primary event vertex,V_z, the Z position at V_x, V_y was calculated for each track. V_z was then the mean of these Z positions where each track was weighted by the estimated error on its Z_0 taken from the FRFT bank.

This algorithm recognizes that there is very little available information about the event vertex in the direction parallel to the event thrust axis, but that the best available information lies in the perpendicular direction. Also, it has no iterative or minimization steps which could be very slow.

Using Monte Carlo simulations of QCD events, shown in figure 7, the width of the distribution in the x direction of the estimated vertex position V_x minus the true V_x is approximately $290\mu m$, while in the y direction the width is approximately $190\mu m$. In the Z direction the tracking resolution is significantly worse, and the width of the estimated V_z minus the true V_z had a width of about $0.8mm$. However, the Monte Carlo does not include the effects of beam jitter which could represent a significant effect in the data and the beam ellipse used has an x-width of $350\mu m$ which is nearly a factor of 2 too large. It should also be noted that because of the beam constraint used in the algorithm there is a substantial correlation between the reconstructed V_x and V_y.

3.1.3 Vertex corrections applied to tracks

Once the tracks which are regarded as 'primary' have been flagged, and the primary event vertex has been found, corrections can be applied to the track extrapolation coordinates at the VDET wafers. These corrections reflect the fact that the tracks need to originate at the primary event vertex, rather than their nominal track positions. Since the track extrapolation coordinates are calculated based on the nominal track fit parameters, two approaches are possible. The 'correct'

method would be to perform a track refit for each track, adding the primary event vertex as another coordinate on the track (with suitable errors). The 'correct' track refit parameters would then be used to calculate the 'correct' track extrapolation coordinates at the VDET. Unfortunately, this method would be very slow.

The method we use does not attempt to alter the track fit parameters, but rather applies a correction to the calculated track extrapolation coordinates based on how much the track would have to be moved at the origin to make it pass through the primary event vertex. The corrections, ΔX, described below are valid in both the $R-\phi$ plane (where the X coordinate can be identified with the VDET local U coordinate) and in the Z direction (where the X coordinate represents the VDET local W coordinate).

This correction is applied by the subroutine VXCONST. As the name implies, this simply forces the track to pass through the primary event vertex. As shown in figure 6B, for the idealised situation of a perfectly straight track (infinite momentum), forcing the track to pass through the primary event vertex is equivalent to adding another point to the track. The effect on the track is to rotate it about a fixed point (probably somewhere in the ITC/TPC) at radius r_{fixed}, and therefore we get the linear correction $\Delta X(r)$ needed at radius r is given by

$$\Delta X(r) = \Delta r_0 \cdot \frac{(r - r_{fixed})}{r_{fixed}}$$

and therefore

$$X_{corrected} = X_{nominal} + \Delta X(r)$$

where Δr_0 is the correction at the event vertex, and r is the radius of the point where the track passes through the VDET wafer. To be more exact, $\Delta X(r)$ is the component of the vector Δr_0 in the VDET's local coordinate frame, multiplied by the radial factor. The value of the unknown quantity r_{fixed} can be determined from the data by making a two-dimensional plot of $\Delta X(r)$ versus the VDET residual (coordinate of track extrapolation at VDET minus coordinate of associated VDET hit). The optimal value of r_{fixed} is that which makes the major axis of the distribution have an angle of 45° to the horizontal axis. In practice, the optimal value of r_{fixed} was found to be $30cm$, about at the ITC/TPC boundary.

The correction is then added to the existing track extrapolation coordinate to give the corrected extrapolation coordinate in the VDET's local coordinate frame. That the correction makes a useful contribution can be seen from figure 9A. The 45° correlation shows that the value of $r_{fixed} = 30cm$ is correct for the U direction correction. The power of the correction is that distribution along the minor axis (vertex-corrected residual) is narrower than the width along the x axis (uncorrected residual). In particular, most of the events in the tails of the raw residual distribution have been brought back into line.

It is also clear from figure 9B that the vertex correction in the W direction is much less powerful than in the U. This probably stems directly from the much larger systematic errors in the TPC Z measurement, which in turn bias the determination of the vertex Z position. Because the improvement here is marginal at best, for the moment we do not apply the vertex constraint correction in the Z direction.

3.2 2-layer and Overlap Techniques

These two methods are very similar, in that they both provide very accurate information about the relative position of 2 wafers. In the overlap method, we consider tracks which hit the overlapping ϕ edges of the wafers, giving a hit on each. In the 2-layer method, we consider tracks which traverse both VDET layers, leaving a hit in each. In both cases the constraint is formed by refitting the track through 1 of the VDET hits associated with the track, and then updating the track extrapolation

point on the other. As in the vertex constraint method, the track is not literally refit and re-extrapolated, but instead a linear correction is made directly to the track extrapolation point on the second wafer. This linear correction is made by the routine VOVRLP, as described in appendix A.

The principle of these techniques is demonstrated graphically in figures 8. We see represented there ITC-TPC tracks, and VDET wafers with hits. By constraining the track to go through the VDET hit in the first wafer, it brings its extrapolation point much closer to the VDET hit in the other.

With this method, the track-hit residual on the second wafer depends most strongly on the relative position of the 2 wafers. Since the extrapolation of the track between the two wafers is done using TPC-ITC track parameters, there is still some dependence on those devices. However, because this distance is very small ($\sim mm$ for the overlap method, $\sim cm$ for the 2-layer method), this dependence is extremely small, and in most cases negligible. In practice, the accuracy of these methods is limited only by the intrinsic resolution of the VDET itself.

This is demonstrated by figures 9 and 10. Here we plot on the X axis the uncorrected residual in the second wafer, with the correction provided by the track constraint to the VDET hit in the first on the Y axis. Figure 9C (9D) shows this correlation in the U (W) direction with 2-layer tracks, as does figure 10A (10B) for the overlap tracks. The linear relation (slope=1) between these demonstrates the correctness of the correction. The narrowness of the diagonal projection (corrected residual) compared to the x-axis projection (normal residual) demonstrates the power of the methods; in the U (W) direction, the resolution is improved by a factor of about 4 (12). The large amount of background in the W direction plots results from misassociation between hits and tracks. Misassociation is much more likely in the W direction than the U because the error on the W track extrapolation is much larger than in the U ($\sim 1mm$ compared with $\sim 150\mu$).

The weakness of these methods is that they only provide *relative* position information, and as such cannot suffice to define the wafer positions relative to the ITC-TPC. However, the methods can be extended to provide more general position information by requiring a *global consistency* to the final result. This is demonstrated graphically for the 2-layer method in figure 11. In figure 11A we see an $R-Z$ view of 2 VDET layers, in figure 11B an $R-\phi$ view of the same. The direct 2-layer method will for instance use tracks like track 1 in figure 11A to get the relative position between wafers C and G. However, since track 2 also goes through wafer G, combining tracks 1 and 2 then provides information about the relative position of wafers C and D. Similarly, combining tracks 2 and 3 provides the relative position of wafers G and H. If we include events with shifted primary vertices, we obtain tracks like number 4, which provides the relative position of wafers F and C. Thus, the relative Z *and* $R-\phi$ positions of all wafers $A-H$ can be obtained.

Switching to figure 11B, we see that this *propagation* of alignment information also works in the $R-\phi$ direction. For example, tracks 5 and 6 together give the relative positions of wafers L and M, etc. If one imagines a detector with a full inner and outer layer, it is easy to see how this principle can be extended to give the relative position of all wafers, IE a complete local alignment. These arguments work equally well using the overlap method.

One flaw with this argument is that the relative position of distant parts of the detector will be poorly understood, as they have been determined with many intermediate steps. One can easily imagine an 'egg shaped' resultant alignment, where all the local constraints hold rigorously, but where the overall shape is wrong. Also, the method breaks down if the detector is not complete. To allow for these possibilities, one must use also the information provided by the vertex constraint and the muon pairs.

A technical difficulty also arises in applying the 2-layer and overlap constraints in this *global* manner, namely that the position of the first wafer (through which the track is extrapolated) must be known in order to use the VOVRLP routine. Of course, only an *approximation* of the first wafer position is known. To avoid this contradiction, we use an *iteration loop*. The loop starts by fixing all

wafers to their *current best known* positions, and calculating the revised track extrapolation point on their corresponding pair member. Note here that the constraint is applied in ***both directions***, IE that a single 2-layer track is used for both the inner and outer layer wafers. All wafer positions are then adjusted according to these new track extrapolations. Any wafer whose position has changed by more than a prescribed amount (see the section on accuracy requirements) is flagged. We then recompute the track extrapolation points by constraining to the new wafer positions, and then solve again for the positions of all flagged wafers. Convergence occurs when no wafer moves outside its allowed window. Typically, this occurs in 3 to 4 iterations.

3.3 Muon Pair Method

Muon pair events provide information on the relative alignment of wafers 180° apart in ϕ and on opposite sides of $Z = 0$. They are thus complementary to the other techniques which have a more "local" scope. An important example is the sensitivity of the muon events to an overall twist of the end rings holding the VDET faces, a non-trivial parameter to control during construction. In general, the muon events should allow us to plug a possible loophole where the 2-layer and overlap techniques, being mainly sensitive to the relative alignment of neighboring wafers, drift into an alignment where there is a smooth deformation across several faces. This can be particularly worrisome if a portion of the detector is dead, thereby preventing the overlap technique from feeding back on itself as one goes around the detector in ϕ. Another motivation for the use of the muon events is our hope that they expose us to systematic effects in the ITC/TPC in a manner "orthogonal" to that in QCD events. The large difference in track multiplicity and curvature between the two event samples gives us some confidence in such a hope. Another important distinction between the muon and QCD events is that in the muon events, each track must go through a different half of the TPC (in effect, two different tracking chambers).

The muon events are taken from the "golden muon sample" of F. Bossi and J. Nash.[1] Selecting muon pairs with an acollinearity angle less than 0.5 degrees, we are left with a sample of 6735 events from the 1990 run. To reduce the statistical and systematic errors from the ITC-TPC system, each muon pair is fit to a single helix. Some idea of the improvement in the statistical precision can be obtained from the following table, based on a very simple Monte Carlo where two back-to-back 45 GeV "muons" are propagated to the radii of the ITC wires and TPC pads and space points smeared by Gaussian distributions with resolutions of $\sigma_{r\phi} = 150\mu m$ for the ITC and $180\mu m$ for the TPC, and $\sigma_z = 1.5mm$ for the TPC.

	$\sigma_{\tan\lambda}$	$\sigma_{\phi_0}(mrad)$	$\sigma_{D_0}(\mu m)$	$\sigma_{Z_0}(\mu m)$
Single muon	7.9×10^{-4}	0.28	87	911
Single helix	2.1×10^{-4}	0.024	30	230

We see an improvement for the single helix fit over the single muon by a factor of 5 to 10.

The systematic effects relevant to the VDET alignment involve the slope and intercept of each muon - four degrees of freedom. Assuming that the two muons are produced back-to-back, the single helix fit constrains two of these.[2] We are then left with two degrees of freedom, the azimuthal angle of the track, and its intercept. Since we are interested in the relative alignment of the VDET wafers, we can constrain the helix to pass through the hit on one wafer, thereby removing another degree of freedom. We chose to constrain the helix to go through the VDET hit associated with one muon leg by *translating* the helix sideways, using the routine VOVRLP (see Appendix A), and then looked at the residual with respect to the hit on the other leg. This is illustrated in Figure 8C. This choice

[1] ℵ Muon Group, ALEPH 90-190, PHYSIC 90-117.

[2] On an event-by-event basis, initial- or final-state radiation will sometimes cause the muons not to be exactly back-to-back. However, they will be back-to-back on average so that we do not expect any systematic bias if we have adequate statistics.

is supported by the data, which show that it results in a narrower residual distribution than by constraining the helix to the VDET hit by *rotating* the track about the origin. In this manner the relative alignment becomes insensitive to the intercept error (both statistical and systematic) of the single helix fit. However, we must rely on the accuracy of the fit for the remaining angular degree of freedom and will necessarily be sensitive to systematic errors on this quantity. To reduce this error, the momentum of the single helix is constrained to the beam energy.

4 Alignment Code

The VDET alignment code is divided into 2 basic programs. The first is an ALPHA program (RESIDUAL), which selects events, tracks, and VDET hits, and outputs these to an NTUPLE. The NTUPLE contains the positions of the track extrapolations and the hits, as well as accessory information such as track direction. The second (ALIGN) is a standalone program which reads in RESIDUAL NTUPLEs, and calls MINUIT to fit for the VDET alignment constants. ALIGN produces directly the alignment bank card files necessary for VDET reconstruction, as well as test histograms.

4.1 Program RESIDUAL

RESIDUAL is made to process events having reconstructed VDET hits (VDXY,VDZT banks), and tracks fit *without* using the VDET points (FRFT,FRTL banks). Its basic job is to select good QCD events, find good tracks in those events, and associate good VDET hits with those tracks.

For each run RESIDUAL unpacks from the JSUM bank the correction to the TPC T0, using a routine supplied by Stephen Haywood. For the 1990 run, the run-by-run T0 correction was measured but not applied. These shifts, which are typically $\sim 1mm$, are applied by RESIDUAL.

Each event, RESIDUAL uses the tracks to determine the primary vertex, as described in section 3.1. If no acceptable primary vertex is found, the event is rejected. Tracks which do not come from the primary vertex are locked from further analysis by XLOCK.

The remaining tracks are then refit using the latest version of the Kalman filter code, provided by Thomas Lohse. This latest version (Jan 1991) has fixed a bug in the calculation of multiple scattering, and thereby removes problems seen with the $Z0$ errors. This bug fix affects only slightly the track parameters themselves. This bug was present in the November 1990 DST-DST reprocessing.

RESIDUAL calls the ALEPHLIB routine VTRKEX, which extrapolates the new FRFT,FRTL tracks onto the VDET crystals, giving a point in the local coordinate system. The Z position of the track extrapolation point is then adjusted for the T0 shift, by subtracting from tracks with $Z > 0$ and adding to tracks with $Z < 0$. Tracks with an ambiguous T0 correction (IE tracks which pass through the TPC septum) are removed.

In extrapolating the tracks, one must use a preliminary version of the VDET alignment. This should be reasonably accurate, as the changes to the alignment are computed using linearized routines (IE which assume no track curvature, with first-order approximations). If this initial alignment file is later found (using ALIGN) to be grossly incorrect (IE wafer positions shifted more than $\sim 1mm$), RESIDUAL should be rerun with the new, improved alignment, and the procedure repeated.

A final set of track cuts is then applied. First, tracks are required to have a momentum $P > 1.0$ GeV, have ≥ 4 ITC and ≥ 6 TPC hits, and a fit $\chi^2/DOF < 4.0$. A further cut is made on track density, to limit the ambiguous situations before making hit associations. Track density is measured in the wafer frame. Tracks whose nearest neighbor in U (W) is $< 500\mu$ ($< 1mm$) are rejected.

Accepted tracks are matched with hits using a trivial 'closest hit' algorithm. Any hit within $1mm$ ($5mm$) in the U (W) direction of a track extrapolation point is taken as a match. If more than one such match exists, the closest hit is taken. Note that the associations are made *separately* in the U and W direction. This separation between directions is maintained throughout the alignment code (IE also in ALIGN). Any track with a matching hit in either direction is recorded in the NTUPLE. In cases where only a single direction is matched, the track error in the missing direction is multiplied by -1, to serve as a flag for ALIGN.

When making the track-hit match, and when entering the track extrapolation point into the NTUPLE, the vertex constraint correction is applied to the U coordinate. Because of poorly understood systematic problems in the TPC, we do not yet trust the vertex reconstruction in the Z direction, and consequently do not correct the track extrapolation point in the W (local Z)

direction. Thus, the NTUPLE data used by ALIGN already has the vertex constraint applied. In the case that the track is later used by ALIGN in a VDET constraint (2-layer constraint, etc), the vertex constraint will simply be overwritten by the much more accurate VDET information.

RESIDUAL in fact stores 3 separate but identically structured NTUPLES. NTUPLE 1 is used to store tracks matching in only a single VDET wafer. NTUPLE 2 stores tracks which match in 2 wafers of the same layer, IE overlaps. NTUPLE 3 stores tracks which match in different layers, IE 2-layer tracks. To be entered into NTUPLES 2 and 3, the hits in the different wafers are required to match in the same dimension (IE UU, WW, or both). The two hit-track pairs are stored sequentially.

ALIGN takes the information for fitting directly from the RESIDUAL NTUPLE. However, the NTUPLE can of course be examined directly using PAW, by which means many bugs and tracking effects have been discovered and examined (such as the Kalman filter problem mentioned above). In addition to the track extrapolation points and errors, and the hit positions, the NTUPLE also contains the track momentum vector, and the run, event, track, and wafer numbers.

4.2 Program MURES

MURES is a version of RESIDUAL slightly modified for the muon pair events. As for RESIDUAL, MURES assumes that the events contain reconstructed VDET hits and that the tracks have been fit without using the VDET hits. The function of the program is to refit the muon pair to a single helix, applying a momentum constraint, associate good VDET hits with the track, and then to fill an ntuple with information on each pair of track-hit matches (one from each muon leg).

The input events are assumed to be good clean dimuon events. The only cut which is applied demands that the acollinearity angle between the two muons be less than 0.5 degrees. After correcting the TPCO coordinates for the t_0 shift, the two tracks are fit to a single helix using the ALEPHLIB 'circle-plus-line' fitter, UFITZS; multiple scattering effects are ignored. The momentum of the resulting track is constrained to the beam energy using a procedure[3] which uses the correlation between the curvature, ϕ_0, and $\tan\lambda$ in the track error matrix to tweak the track parameters so that the momentum is fixed to the beam energy.

The rest of the program is essentially identical to RESIDUAL. The single helix is extrapolated to the VDET wafers, and matched to VDET hits with the same cuts as in RESIDUAL. If both legs of the single helix have VDET hits matching in the same dimension, the track-hit pairs are stored in an NTUPLE; the NTUPLE is numbered 4 to distinguish it from those created by RESIDUAL.

4.3 Program ALIGN

4.3.1 Overview

The program ALIGN is a standalone program that uses HBOOK routines to read in NTUPLEs created by RESIDUAL and MURES, and calls MINUIT to fit for the data. The program is controlled with a simple menu interface, and can be run in batch. The main purpose of the code is to process and pack the data from the NTUPLES into local arrays, which are then used by a χ^2 function called by MINUIT. All 4 of the local alignment techniques use the same data structure and the same χ^2 routine. This universality is a key program feature, and is what allows the methods to be applied simultaneously.

4.3.2 Data Flow

The basic dataflow of ALIGN is simple. NTUPLE data is read in and unpacked into local arrays. Separate arrays hold identical information for each of the 4 NTUPLEs, consisting of the track

[3] J.P. Berge et al., Rev. Sci. Inst. 32 (1961) 538.

extrapolation point, the errors on that point, the track momentum vector, and the VDET hit point.

This information is not directly used to calculate alignment. Instead, for each iteration of the alignment, these 4 sets are copied into a single set of arrays. In the copying, the requested constraints are applied, and the track extrapolation points and errors appropriately modified. The VDET hits are never modified; since they were measured in the local co-ordinate system to begin with, they are by definition correct. Thus, the alignment is driven by the *combined* data from each of the 4 techniques in a natural way.

VDET data constraints are applied using the routine VOVRLP (see appendix A). In all cases, the constraint is applied by correcting the track extrapolation point in one wafer given the track extrapolation point and the VDET hit point in the other. In filling the final arrays for the alignment fit, the constraints are applied in *both directions*; IE, a single 2-layer track is entered twice, once constrained at the inner layer and projected to the outer, once constrained at the outer layer and projected to the inner.

In addition to applying the constraints, a track selection is performed while copying the separate NTUPLE data into the common arrays. These cuts remove tracks which are very far from the hit point, thus removing the background due to mis-association in RESIDUAL. These cuts are renewed each iteration, as the knowledge of the wafer position improves. However, the set of hit-track pairs used in the alignment remains fixed during the iteration.

To create the final data sample for the vertex constraint, both NTUPLEs 1 and 2 are unpacked. This ensures that the vertex constraint data is not biased to sections of the detector which lack an outer (or inner) layer.

4.3.3 Main menu

The main menu of ALIGN contains the following entries:

Global alignment: This takes the data in the common blocks and performs the global alignment. Only wafers on a (pre-set) list are considered. No constraint techniques are used. Only hits within $\mathcal{N}\sigma$ of the associated track (using the starting local alignment positions) are used. The data preparation is done by the routine GLOBAL. The χ^2 is calculated by the function GLOBALCHI, which is called by MINUIT. This is computed as the sum over all selected track-hit pairs from all wafers of the square of the residual divided by the track error;

$$\chi^2 = \sum_{wafers} \left(\sum_{U\,pairs} \left(\frac{U_{VDET} - U_{track}}{\sigma_{U_{track}}} \right)^2 + \sum_{W\,pairs} \left(\frac{W_{VDET} - W_{track}}{\sigma_{W_{track}}} \right)^2 \right)$$

Each time MINUIT calls GLOBALCHI, the track extrapolation points are adjusted to reflect the instantaneous value of the 6 global alignment constants. This is done in a two-stage process, whereby the 6 constants are first transformed into equivalent *local* alignment constants, and then the track extrapolation positions are adjusted by the routine VNEWEX (see appendix B).

Local alignment: This takes the data in the common blocks and performs the local alignment. This makes a loop over all wafers, either singly or grouped according to module or face. All wafers (or module or face, depending on choice) having $\geq N_U\,U$ hits or $\geq N_W\,W$ hits are considered. If requested, the data samples from the constraint techniques (overlap, 2-layer, and muon pair constraints) are included into the list of final hit-track pairs. In applying the constraints, the *current best* wafer positions are used. Only hits within $\mathcal{N}\sigma$ of the associated track (using the *current best* alignment positions) are used. If the track error was overwritten by a constraint technique preparation, that is the error used in making this cut. The data preparation is done by the routine LOCAL. The χ^2 is calculated by the function LOCALCHI,

which is called by MINUIT. This is computed as the sum over all selected track-hit pairs of the square of the residual divided by the track error:

$$\chi^2 = \sum_{U\,pairs} \left(\frac{U_{VDET} - U_{track}}{\sigma_{U_{track}}} \right)^2 + \sum_{W\,pairs} \left(\frac{W_{VDET} - W_{track}}{\sigma_{W_{track}}} \right)^2$$

Each time MINUIT calls LOCALCHI, the track extrapolation points are adjusted to reflect the instantaneous value of the 6 local alignment constants for that wafer, using the routine VNEWEX (see appendix B).

Set parameters: This transfers control to a sub-menu, where all the important parameters used in the alignment procedures can be examined and changed.

Write histograms: This fills a set of diagnostic histograms, and writes them to disk. Normally, this is called after alignment, but it can also be used standalone to test a new alignment file. New alignments are entered in the form of card files, as described below

Write alignment: This creates a card file of the VDET alignment banks VAGB and VALC (global and local, respectively) from the current best alignment held in memory, and writes this to disk. This card file can later be read back by ALIGN (see below). It can also be used for a RESIDUAL job, or entered directly into the database to define a new alignment for the reconstruction.

Read NTUPLE: This reads in an NTUPLE file, as produced by RESIDUAL. Any of the 4 NTUPLEs (1,2,3, or 4 for vertex constraint, overlap, 2-layer, and muon hit-track pairs respectively) present on the file will be unpacked, and entered into the appropriate local arrays. This can be called repeatedly to accumulate statistics from different files. However, all files must have been created using *the same VDET alignment*, as described below.

Read alignment: This reads in 2 sets of VDET alignment constants, in the form of card files for the VAGB and VALC banks. The first *must* be the alignment card file used to create the RESIDUAL NTUPLEs. Consistency between these banks is *essential* if the results of ALIGN are to make any sense. The second set of bank cards can have any value desired, but should in general be the best currently known VDET alignment (which may not have been available when RESIDUAL was run). The difference between the 2 alignments defines the starting values for the local variables used to define the change in alignment during the minimization. Of course, this second bank can be the same as the first, in which case the initial values in the minimization will all be zero.

4.3.4 Set Parameter Menu

This menu allows one to fine-tune the alignment procedure cuts interactively. The entries available are:

Minimization mode: This defines whether MINUIT is called in its normal form, or its interactive form. The interactive form is useful for debugging. A mode also exists for calculating the MINOS error correlation matrix, which can be called after normal convergence.

Match σ: This defines the cut on the track-hit separation in terms of the number of σ of the track error. This is separated U and W.

Alignment mode: This defines which of the 4 alignment techniques will be applied. Any combination is allowed.

Minimum hits: This defines the minimum number of matched hit-track pairs per wafer to attempt alignment. This cut is applied separately in the U and W direction.

Track σ limits: This defines a window around the track errors as projected to the VDET wafer, separately in the U and W directions. Tracks with errors outside this window are rejected in the alignment fit.

U, W flags: These flags allow one to restrict the χ^2 calculation to use information only from a single dimension. This is mostly for debugging.

Parameter flags: These flags allow one to fix some of the 6 degrees of freedom allowed in the wafer alignment minimization. This is mostly for debugging.

Iteration setup: This sets a value for the maximum number of iterations. Also here is determined whether the minimization is done by wafer, module, or face.

Wafer limits: This limits the range of wafers used in the local alignment. This is mostly for debugging.

Constraint σs: This defines the values used to overwrite the track errors in the various VDET data constraint techniques.

Event fractions: This allows one to adjust the relative composition of a data sample between the 4 different constraint techniques. If one of the values is set less than 1.0, then only that fraction of the available hit-track pairs from the given technique will be used. These are selected randomly.

5 Results from 1990 data

The alignment procedures described in this note were developed by running on the 1990 data. The final results display a high degree of self-consistency, which encourages us to believe that the techniques are valid. While we plan to test the techniques with Monte Carlo data in the 1991 VDET configuration, we believe that the success of the 1990 alignment both proves the methods, and provides a VDET alignment of adequate quality.

5.1 General VDET Performance in the 1990 Run

This section describes some basic features of the VDET performance during the 1990 run. This information defines the conditions under which the alignment code operated.

Figure 12 is a timeline of the 1990 LEP run, displaying the fill number vs date. The vertical lines on the graph delimit the detector access periods; solid lines note periods where the endcaps were opened, dashed lines where they remained closed. Thus, ALEPH was opened 10 times during the run. Because the 90 VDET was attached to the beampipe, and not directly to the other tracking devices, it was feared that it might have moved relative to the other detectors, especially when the endcaps were opened. To search for possible VDET movement, we therefore divided the run up into 10 periods, delimited by detector openings.

During the earliest run period, the VDET was not in the DAQ; we ignore those fills. In the subsequent run period (1), cooling problems prevented us from powering the entire outer layer. This period was the least noisy of the entire run. In periods 2 and 3 all working VDET wafers were powered. The data from these periods was very noisy. Also during these periods, some online bugs were discovered and fixed, which improved the efficiency. Towards the end of period 3 automatic pedestal updating was installed, which reduced the noise. During the access before period 4, a power failure destroyed some 20% of the VDET faces. The VDET remained out of the DAQ all through period 4 while safe power was being established. From then on, the VDET ran smoothly, with a large but tolerable noise level.

Figures 13 A and B shows a plot of the single coordinate VDET efficiency (U and W separately) from a fill in period 8. This is measured by counting the number of times a track which projects into the active area of a VDET wafer has a matching hit. As can be seen, the efficiency varies strongly across the detector. This variation biases the alignment, giving more weight to regions with high efficiency. Figures 13 C and D show the signal/noise for the detectors, defined as the sum pulseheight of clusters divided by the noise on a single strip. The average values of ~ 10 correspond approximately to the testbeam numbers.

5.2 VDET motion

To test for VDET motion, we ran the alignment on samples of 10K hadronic Z_0 decays from each period. Because the VDET data constraint techniques provide only *relative* wafer position information, those were not used in this test; only the vertex constraint technique was applied. This of course compromised the accuracy of the absolute position measurements, but still allowed an accurate comparison to look for changes in position. Because the alignment uses the TPC-ITC tracks to define the absolute position of the VDET, this test was *insensitive* to motion smaller than the precision of those devices ($\sim 100\mu$ in U and $\sim 1mm$ in W). Beyond this limit, the absolute VDET position is *meaningless*, having no effect on the alignment or the physics. However, the *relative* position of the wafers is relevant down to a much finer scale.

Figure 14 plots the difference between wafer positions found from periods 5 and 9, separated into radial, U, and W directions. Each plot contain numerous entries for each wafer which was working in both periods. The entries for each wafer come from comparing the relative positions

of uniformly distributed points across the wafer as calculated using the different alignments. This technique is also used in subsequent comparisons.

Because these distributions center at zero, we believe that the *global* VDET position relative to the TPC-ITC did not *measurably* change. For instance, if the detector had rotated about the Z axis, the U plot would not be centered. The structures seen in the W direction correspond in magnitude to the expected T_0 shifts and distortions. Discrepancies of this magnitude do not appear when VDET constraint techniques are used in the alignment. This fact is demonstrated below, in the muon pair comparison section.

The width of these distributions should measure the relative motion of VDET wafers. This width is however inconsistent with the statistical errors given by the alignment fit, as demonstrated in figures 14D-F. The extra 50 % in width should in principle be interpreted as VDET relative motion: 20 μ in U, 180 μ in V (we consider the width in W as coming from TPC systematics). However, this same 50% increase is also seen when comparing any two run periods, and even when comparing *2 adjacent fills*, with all detector and running conditions unchanged in between. Motion on this short time scale seems very unlikely, especially since it is non-cumulative (the discrepancy being equal between 2 days and 6 months). It seems more likely that instead, the errors given for the TPC-ITC tracks in the FRFT bank are *underestimated*, which would propagate into an underestimation of the error on the VDET alignment. This assumption is corroborated by more accurate results presented ahead, where the errors are taken from measured distributions. We therefore tentatively conclude that the VDET was stable during the 1990 run.

5.3 Final 1990 Alignment Determination

To produce the final alignment constants for the 1990 run, we chose a set of $\sim$ 20K Z_0 events, with 5K from period 1, and 15K from period 9. This combination contains data from all VDET wafers which ever took data in 1990. Added to this were all the muon pair events (800 U, 600 W events), and all the overlap tracks (1600 U, 550 W tracks) from the entire run. The muon pairs were found almost exclusively in the vertical plane, because the wafers in the horizontal plane were dead for most of the run. Overlap tracks were found only in the 4 outer faces of sector 3. Elsewhere, the geometry and active area of the wafers provided *no overlap*.

The alignment was run on all wafers having at least 50 hit-track pairs. Typically, there were about 500 pairs for each wafer. All of the constraint techniques were applied. To remove the influence of the biased Z position given by the raw TPC tracks, these were not used. A cut of 3 σ was applied to the match between hits and tracks.

In running the alignment, it was discovered that the data contained no tracks which crossed $Z = 0$ in going from the inner to outer layer (see track 4 in figure 11). Without these tracks, and without a bridge of working detectors between the upper and lower halves, we were unable to determine the relative Z position of the A and B halves of the detector. This single number was then taken from an optical measurement of sector 3, and propagated to the other sectors using the muon pairs. This optical measurement will be discussed in a future note.

Figures 15-18 plot the residual distributions after the final alignment for each of the 4 constraint techniques. In particular, note that all 3 of the VDET constrained techniques have achieved essentially the same resolution: $\sim 40\,\mu$ in U, $\sim 60\,\mu$ in W. This indicates that the alignment has found a solution where all of the techniques are equally well satisfied. This consistency is non-trivial, as the connection between the constraint techniques occurs only through the iteration step of the alignment.

The absolute values of these numbers however are inconsistent with the expected VDET resolution. If we assume the resolution of the constraint techniques is dominated by the VDET statistical resolution (which theoretically it should be), we obtain a resolution of $\sim 28\,\mu$ in U, and $\sim 42\,\mu$ in W. The discrepancy between these numbers and the resolution from the testbeam can either be interpreted as additional noise in the ALEPH VDET, problems with the TPC-ITC tracking, or

unknown effects in the VDET (such as magnetic field effects on the charge collection, which was not studied in the testbeam). The discrepancy can not be due to misalignment, as the relative wafer positions were free parameters in making the plots.

5.4 Alignment Error Analysis

5.4.1 Statistical errors

Figure 19 plots the statistical errors averaged over the wafer face, in the V, U, and W directions. Each entry in each plot comes from a single wafer. Drawn over these are the accuracy limits prescribed in table 3 for the 1990 geometry. As can be seen, most of the wafers meet the necessary requirement on statistical accuracy. The wafers that fail are mostly isolated detectors with a very poor efficiency. To avoid the effects of the wafers in the tails, we define the average statistical error as the most likely value in these plots.

5.4.2 Technique comparison

To estimate the systematic errors, we compare the final alignment position with that favored by the individual constraint techniques. Figures 20-21 plot, by wafer, the average U and W positions for each of the 4 techniques, relative to the final alignment position. The error bar is the statistical error on the mean. As can be seen, the techniques generally agree very well within their statistical limits. The only exception is the normal W, where the wafers disagree substantially. As previously mentioned, we believe this to be due to TPC systematics, and not a problem with the VDET alignment.

To quantify this, figures 22A and B plot the projection of figures 20 and 21 (IE the difference between the VDET constraint techniques and the final alignment) onto their Y axis. We then interpret the *width* of these distributions as the systematic error on the alignment; this gives ~ 7 μ in U, ~ 15 μ in W. It should be emphasized that these widths are consistent with the *statistical errors* of the individual measurements. This is demonstrated in figures 22C and D, where the values from figures 22A and B have been divided by their statistical error. These normalized distributions have a width of ~ 1.

5.4.3 Reproducibility test

To test the reproducibility of the alignment algorithm, we re-ran the code starting from a randomized initial condition. To randomize, we started with the final wafer positions, and distributed the 6 parameters for each wafer about this value by a gaussian of width 5 $\times$ the statistical error on that parameter. In addition to this scattering, a *global* offset to each of the six parameters for each wafer was introduced. These offsets were also chosen randomly from the same gaussian distribution described above.

From this starting point, the alignment was run as described above, on the identical data sample. Figures 23A-C plot the differences between the final alignment and the alignment from the random starting point, using the usual uniform-point method. Gaussian fits give widths of 4 μ in the U direction, 22 μ in the V, and 13 μ in the W direction. No statistically significant offsets are seen. Normalizing these differences to their statistical error, we see in figures 23D-F a spike at 0 of width $< 1.$, as we expect when comparing correlated measurements.

5.4.4 Independent sample test

As another systematic test, we ran the alignment on a statistically independent sample of data. This second sample had an equal number of normal vertex constrained tracks and 2-layer tracks. Unfortunately, due to their scarcity, it was impossible to separate the muons or the overlap events

Table 4: Alignment errors

Error type	V error μm	U error μm	W error μm
Statistical	38 ± 35	6 ± 5	15 ± 21
Technique Comparison	no information	7	15
Reproducibility	22	4	13
Total	$38 \oplus 22$	$6 \oplus 7$	$15 \oplus 15$
Tolerances	61	20	24

into two samples. Thus, these were excluded from this test, somewhat compromising the clarity of the interpretation of the results.

Figures 24A-C plot the difference between the final alignment and the alignment from the independent sample, using the usual uniform-point method. Gaussian fits give widths of 15 μ in the U direction, 66 μ in the V, and 22 μ in the W direction. No statistically significant offsets are seen. Figures 24D-F plot the same differences, divided by their statistical errors. The widths of these curves are ~ 1, showing that the distributions are consistent with statistical errors. A 25 % excess in width for the U normal distribution could be related to the problem with fit errors shown earlier. If interpreted as a systematic error, it gives a value of 9 μ. The W normal distribution has a width $< 1.$, indicating a correlation between the two samples. This is a known effect, resulting from the lack of any information in this test tying together W positions of distant parts of the detector. In the final alignment, this information is provided by the muon pairs. In the U and V directions, this connection is provided by vertex constrained tracks as well as the muons, and so the same effect is not seen in this test.

5.4.5 Conclusion

Given the available techniques, we have estimated the statistical and systematic errors on the alignment. These numbers are summarized in table 4. Also in this table are tolerances on the translation parameters from table 3.

5.5 Muon Miss Distance

As a final test of the alignment, we refit the muon pair events (each branch separately) including the aligned VDET point, and compare the miss distance between these tracks at the origin. The latest Kalman filter code (Jan. 1991) is used. Figure 25A shows the distribution of the sum[4] of the impact parameters for muon pairs where each muon has been refit with one or more VDET hits in the $r-\phi$ dimension. A Gaussian fit gives a σ of $57\mu m$, corresponding to a resolution of $\sim 40\mu m$ for a single muon. Figure 25B shows the distribution of the difference of the Z_0 between the two muons, with a σ of $73\mu m$ which corresponds to a resolution of $\sim 52\mu m$ for a single muon. By constraining the momentum of each muon to the beam energy in the fit, the $r-\phi$ impact parameter resolution is further improved as shown in Figure 25C, which has a σ corresponding to a resolution of $\sim 37\mu m$ for a single muon; no improvement is seen or expected in the z direction.

The effect of the various constraint techniques on the alignment is shown in figures 26 through 28. Figure 26 shows the muon miss distance if one aligns the VDET without the muon pair events. Figure 27 shows the case where one removes in addition the overlap constraints and the 2-layer constraints (i.e. only the vertex constraint is applied). Finally, Figure 28 shows the case where no constraints are applied at all. This is the situation where the TPC-ITC systematic errors are fully propagated to the VDET alignment.

[4]It is the sum which is relevant here because of the sign convention for the impact parameter.

Table 5: Dimuon data refit results

	Without mom. constraint		With mom. constraint	
Alignment constraints	$\sigma_{\Sigma D_0}(\mu m)$	$\sigma_{\Delta Z_0}(\mu m)$	$\sigma_{\Sigma D_0}(\mu m)$	$\sigma_{\Delta Z_0}(\mu m)$
All four	56.9 ± 2.2	72.8 ± 3.2	51.6 ± 2.0	72.8 ± 3.3
Vertex+overlap+2 layer	65.9 ± 2.8	112.8 ± 7.5	56.0 ± 2.4	113.4 ± 7.4
Vertex constraint only	70.9 ± 2.5	668.0 ± 25.4	63.4 ± 2.3	665.4 ± 25.5
No constraints	76.4 ± 2.8	not fit	67.7 ± 2.5	not fit

Table 6: Dimuon Monte Carlo refit results

	Without mom. constraint		With mom. constraint	
	$\sigma_{\Sigma D_0}(\mu m)$	$\sigma_{\Delta Z_0}(\mu m)$	$\sigma_{\Sigma D_0}(\mu m)$	$\sigma_{\Delta Z_0}(\mu m)$
test beam resolution	41.6 ± 1.2	42.5 ± 1.3	25.4 ± 0.9	42.4 ± 1.4
Aleph resolution	59.1 ± 1.7	73.7 ± 2.2	45.5 ± 1.4	75.0 ± 2.3

The sigmas of these distributions are summarized in table 5; these give some indication of the magnitude of the systematic effects present in the ITC-TPC system. For instance, subtracting in quadrature $1/\sqrt{2}$ of the widths with no constraint from the widths with all constraints estimates the systematic errors as 34 μm in $R - \phi$, and ~ 1 mm in Z.

Note that there is a shift of 30 μ in the D_0 distribution without any constraints. We believe this shift is caused by some global systematic error in the TPC-ITC systems.

A full understanding of how well our final results compare to expectations requires a complete VDET Monte Carlo, and such studies will be carried out soon when the Monte Carlo is in working order. In the meantime, we use the simple Monte Carlo described in Section 3.2 which gives a σ of $42\mu m$ for the sum of the D_0's and $43\mu m$ for the difference in Z_0 for tracks with one VDET hit in the inner layer. These numbers were obtained with a VDET spatial resolution of $13\mu m$ in $r - \phi$ and $16\mu m$ in z, corresponding to resolutions observed in the test beam.

As described above, the spatial resolution of the VDET was measured with colliding beam data to be $\sim 28\mu m$ in u and $\sim 42\mu m$ in w. Plugging these values into our Monte Carlo, a more consistent picture of the alignment results emerges. The results are shown in figure 29 and listed in table 6. We obtain a σ of $59\mu m$ for the sum of the impact parameters and a σ of $74\mu m$ for the Z_0 difference, comparing well with what we observe in the data.

5.6 Muon momentum resolution

We have compared the momentum resolution in dimuon events with and without using the aligned VDET points in the fit. Only tracks with good U hits are considered in this study. Figures 30A and B show the results. We observe an improvement of $\sim 20\%$. This is roughly consistent with the MC model results presented in table 1, which shows that we expect a 25% improvement in the p_t resolution of muon pairs when using the VDET.

6 Conclusion

We have developed alignment techniques which provide a VDET alignment of the necessary statistical and systematic accuracy. This is demonstrated by application to the 1990 data. All of the code was developed using the 1990 data, but should function identically with the 1991 data. In

fact, the techniques developed should work much better with the 1991 detector, because of its full outer layer, increased amount of ϕ overlap, and by having a link of working detectors between all parts of the detector. We therefore expect to be able to align the 1991 VDET immediately after the new detector is producing reliable data, from a sample of some 10K Z_0s.

A Subroutine VOVRLP

This routine is used to provide a correction to the track extrapolation at one VDET wafer based on a VDET hit in another wafer. The typical track extrapolation error can be several hundred microns if only the TPC and ITC tracking information is used (especially for low momentum tracks which have large multiple scattering errors). However, if a VDET hit is available, then the position of the track at that wafer is known to the precision of the VDET ($\sim 15\mu m$). Using this information leads to an enormous improvement in the precision with which the track can be extrapolated to other VDET wafers.

Given that a track passes through two VDET wafers, routine VOVRLP estimates the correction necessary to the track extrapolation at one VDET wafer based on a hit in the other. The two wafers can either lie in a given layer (in which case the track passes through the overlap region between them), or in separate layers.

The routine starts by calculating the residual in the first VDET wafer's local coordinate system (*i.e.* the hit coordinate minus the track extrapolation point). The vector representing this displacement is then transformed into the local coordinate system of the second wafer, by first transforming it into the ALEPH coordinate system. The correction to the track extrapolation is then taken as the projection of this vector into the wafer plane of the second wafer.

In principle, one should use a more sophisticated algorithm for this adjustment, involving the curvature of the track, the different tilt angles of the different wafers, etc. In practice, our attempts to take these effects into account have uniformly degraded the quality of the correction, as measured by the width of the final residual distributions. While we do not understand this, we have taken the empirical evidence to heart, and continue to use our simple, effective algorithm.

B Subroutine VNEWEX

The subroutine VNEWEX calculates the change in the local coordinates of the point at which a track intersects a VDET wafer, given a change in the six alignment parameters. The change in the track direction (expressed in local coordinates) at the intersection point is also computed. To simplify the calculation, it is assumed that the changes in the parameters are small enough that only first order terms need to be kept. This results in no loss of generality as an arbitrarily large change in the parameters can be considered as a succession of sufficiently small changes. However, it does require some caution during the χ^2 minimization procedure. By dropping the higher order terms, we are in the enviable situation where all the displacements commute with one another. The effect of each displacement can be computed individually without having to worry if other displacements have already been performed. Furthermore, since the displacements are small, we approximate the track trajectory by a straight line. With these assumptions, we obtain for the track extrapolation point:

$$\begin{pmatrix} u\prime \\ w\prime \end{pmatrix} = \begin{pmatrix} u - \delta u + \delta v \cdot \frac{p_u}{p_v} \\ w - \delta w + \delta v \cdot \frac{p_w}{p_v} \end{pmatrix} + \begin{pmatrix} -\delta\alpha_w \frac{p_u}{p_v} & \delta\alpha_v + \delta\alpha_u \frac{p_u}{p_v} \\ -\delta\alpha_v - \delta\alpha_w \frac{p_w}{p_v} & \delta\alpha_u \frac{p_w}{p_v} \end{pmatrix} \begin{pmatrix} u \\ w \end{pmatrix}$$

and for the track direction

$$\begin{pmatrix} p_v\prime \\ p_u\prime \\ p_w\prime \end{pmatrix} = \begin{pmatrix} 1 & \delta\alpha_w & -\delta\alpha_u \\ -\delta\alpha_w & 1 & \delta\alpha_v \\ \delta\alpha_u & -\delta\alpha_v & 1 \end{pmatrix} \begin{pmatrix} p_v \\ p_u \\ p_w \end{pmatrix}$$

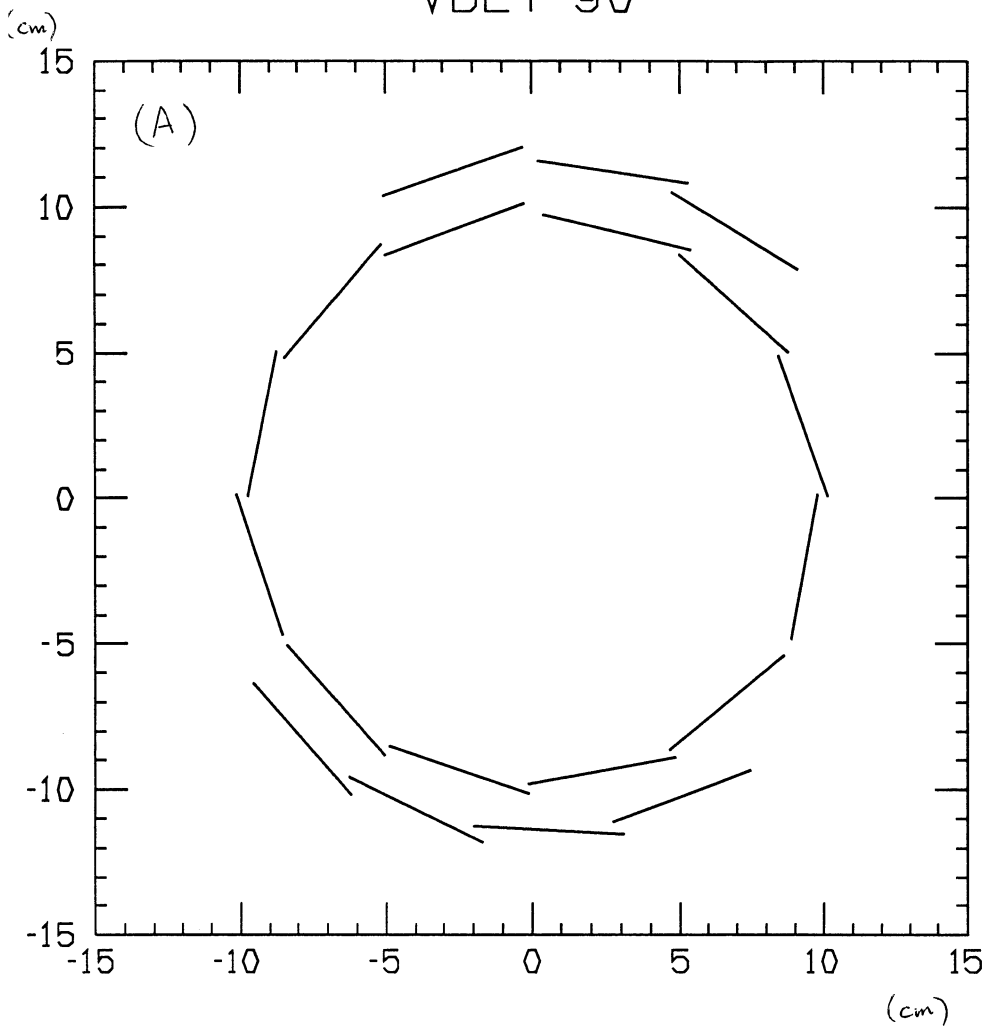
VDET 90
(cm)
(A)
15
10
5
0
-5
-10
-15
-15
-10
-5
0
5
10
15
(cm)

Figure 1

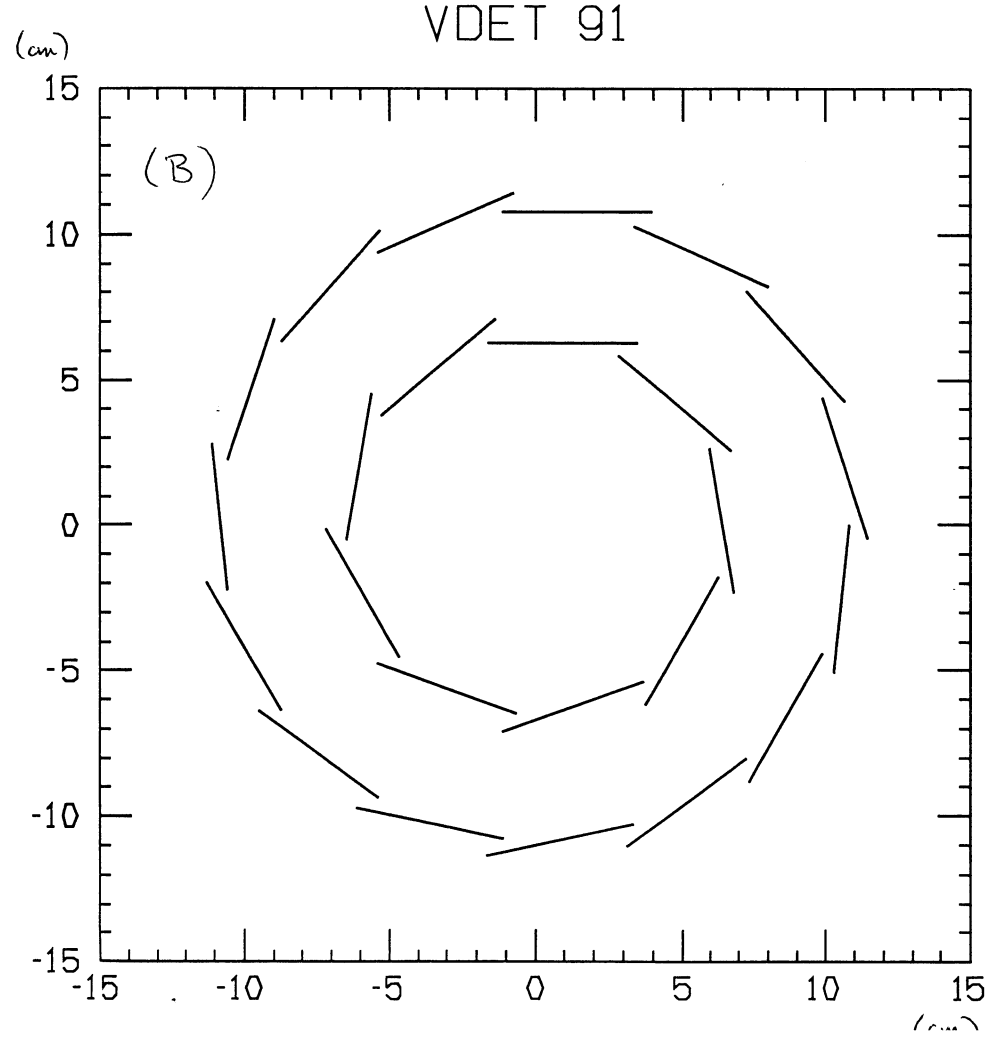
VDET 91
(cm)
(B)
15
10
5
0
-5
-10
-15
-15
-10
-5
0
5
10
15

Figure 2.

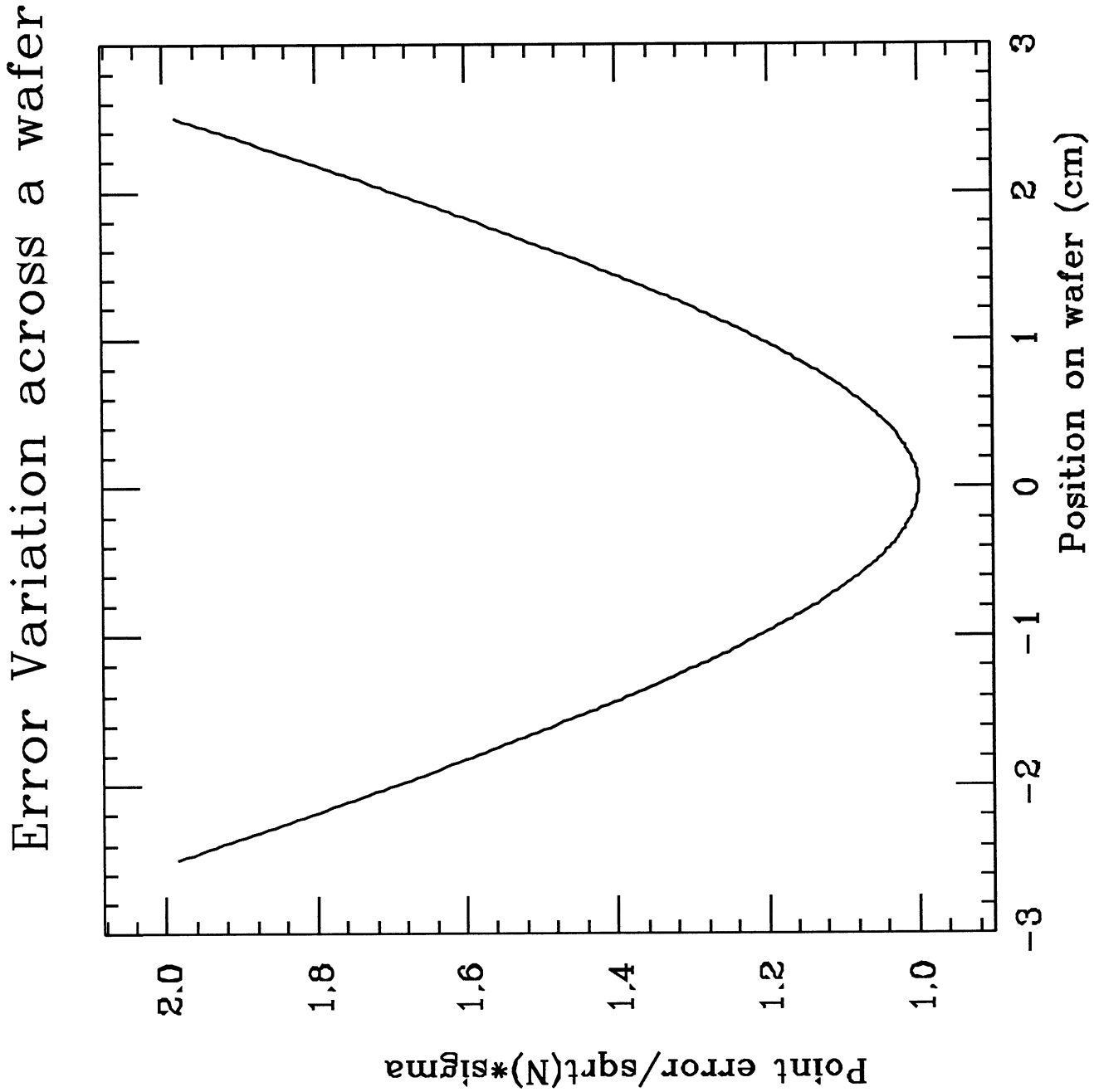
Error Variation across a wafer
Point error/sqrt(N)*sigma
2.0
1.8
1.6
1.4
1.2
1.0
-3
-2
-1
0
1
2
3
Position on wafer (cm)

Figure 3

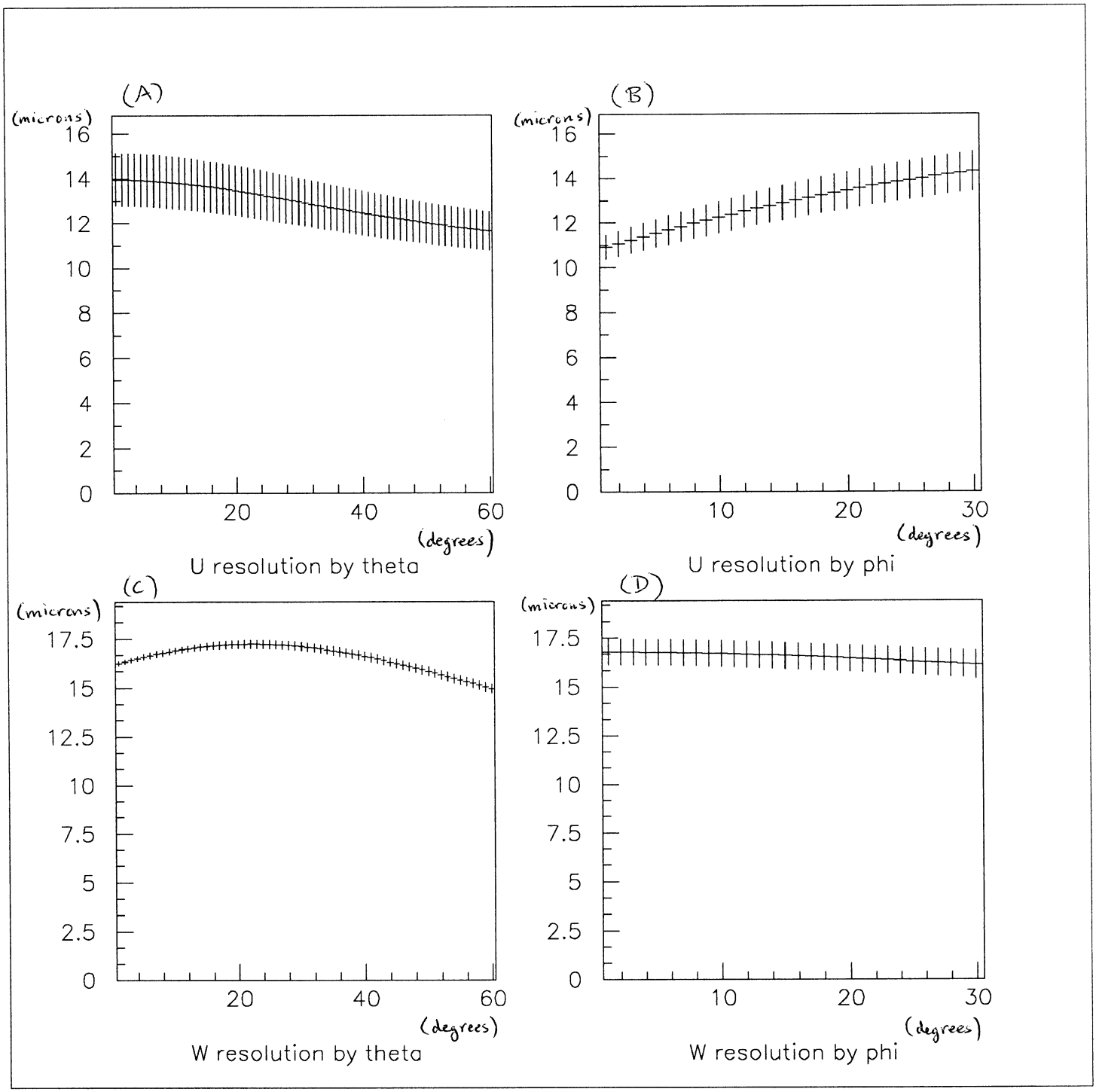
(A)
(microns)
16
14
12
10
8
6
4
2
0
20
40
60
(degrees)
U resolution by theta
(B)
(microns)
16
14
12
10
8
6
4
2
0
10
20
30
(degrees)
U resolution by phi
(C)
(microns)
17.5
15
12.5
10
7.5
5
2.5
0
20
40
60
(degrees)
W resolution by theta
(D)
(microns)
17.5
15
12.5
10
7.5
5
2.5
0
10
20
30
(degrees)
W resolution by phi

Figure 4

Impact Parameter Dependence on Misalignment

Planar translation

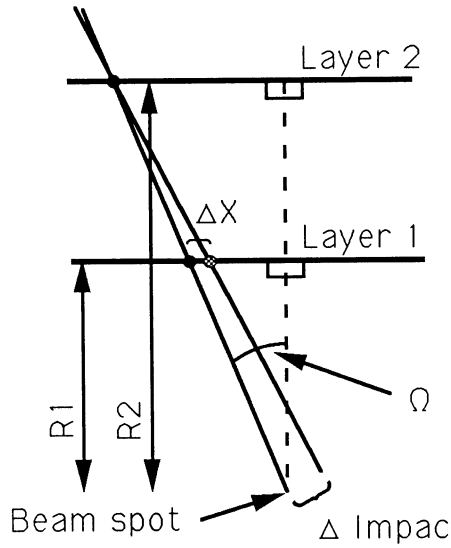

Δ Impact =
R2/(R2-R1) Cos(Ω) ΔX

Planar rotation

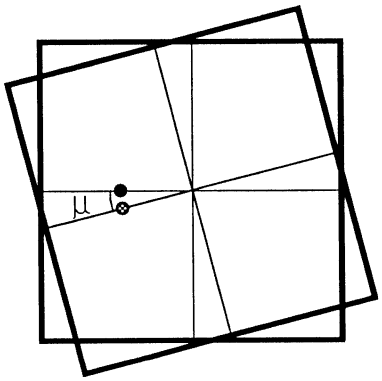

Δ Impact =
R1*R2/(R2-R1) Cos(Ω) Sin(Ω) μ

Vertical translation

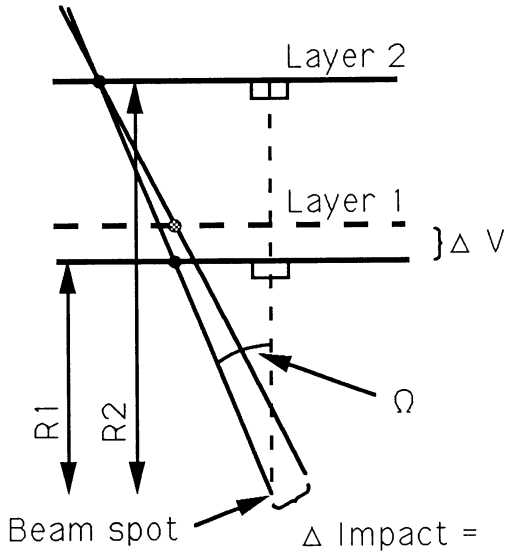

Δ Impact =
R2/(R2-R1) Sin(Ω) ΔV

Out-of-plane rotation

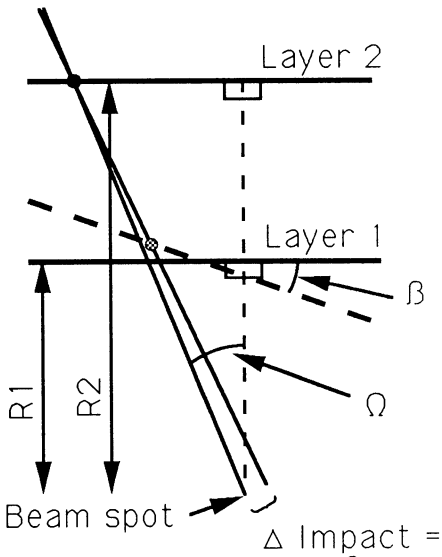

Δ Impact =
R1*R2/(R2-R1) $\sin^2$(Ω) ß

Figure 5

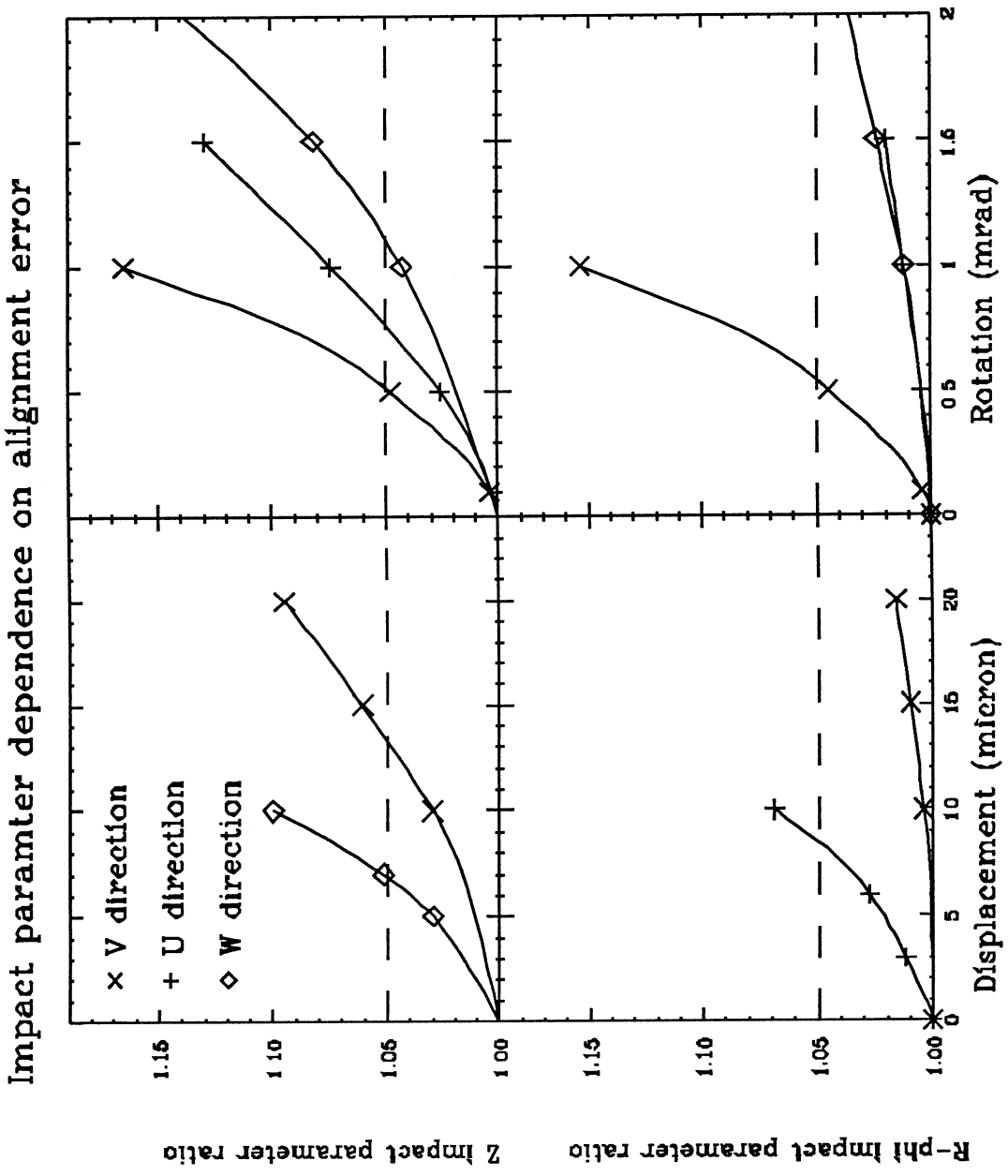
Impact paramter dependence on alignment error
× V direction
+ U direction
◇ W direction
Z impact parameter ratio
R-phi impact parameter ratio
Displacement (micron)
Rotation (mrad)

Figure 6A

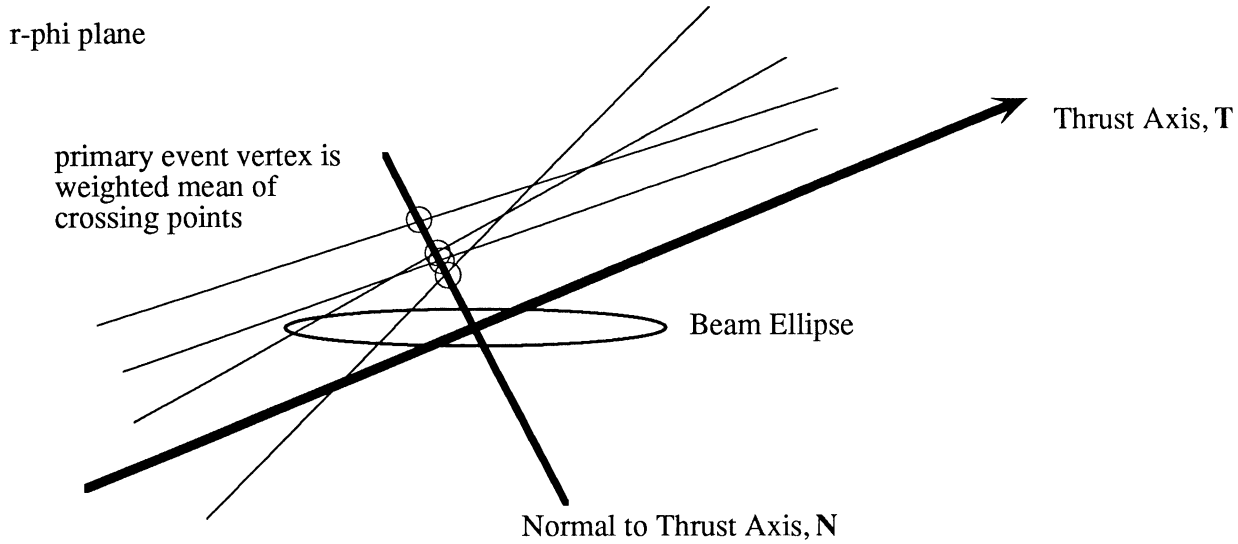

Figure 6B

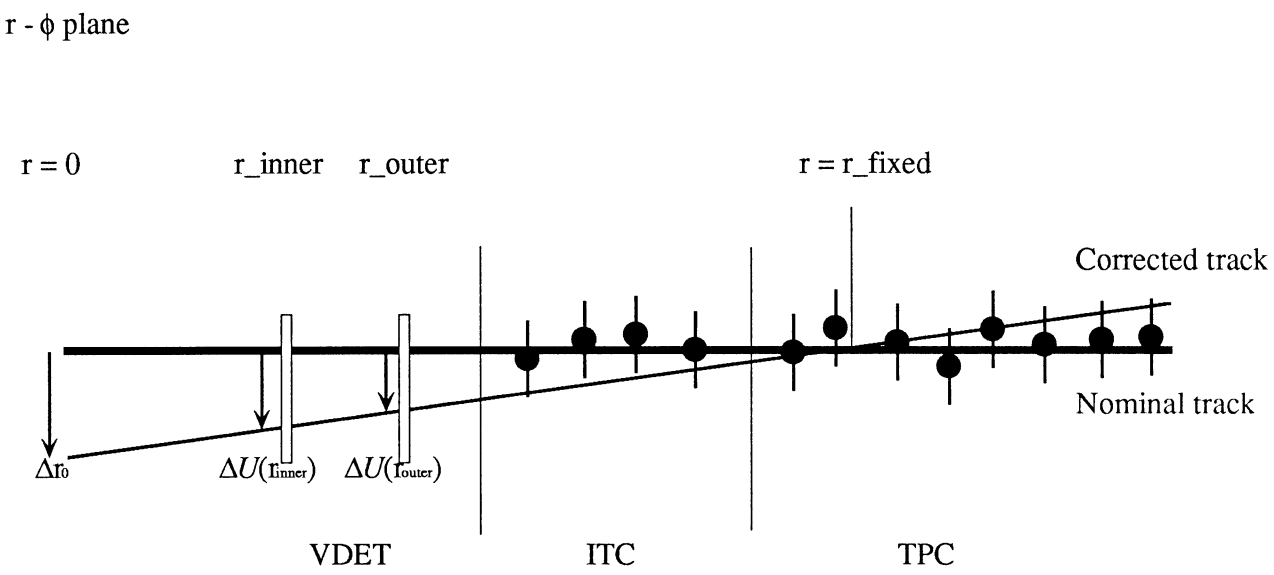

Figure 7

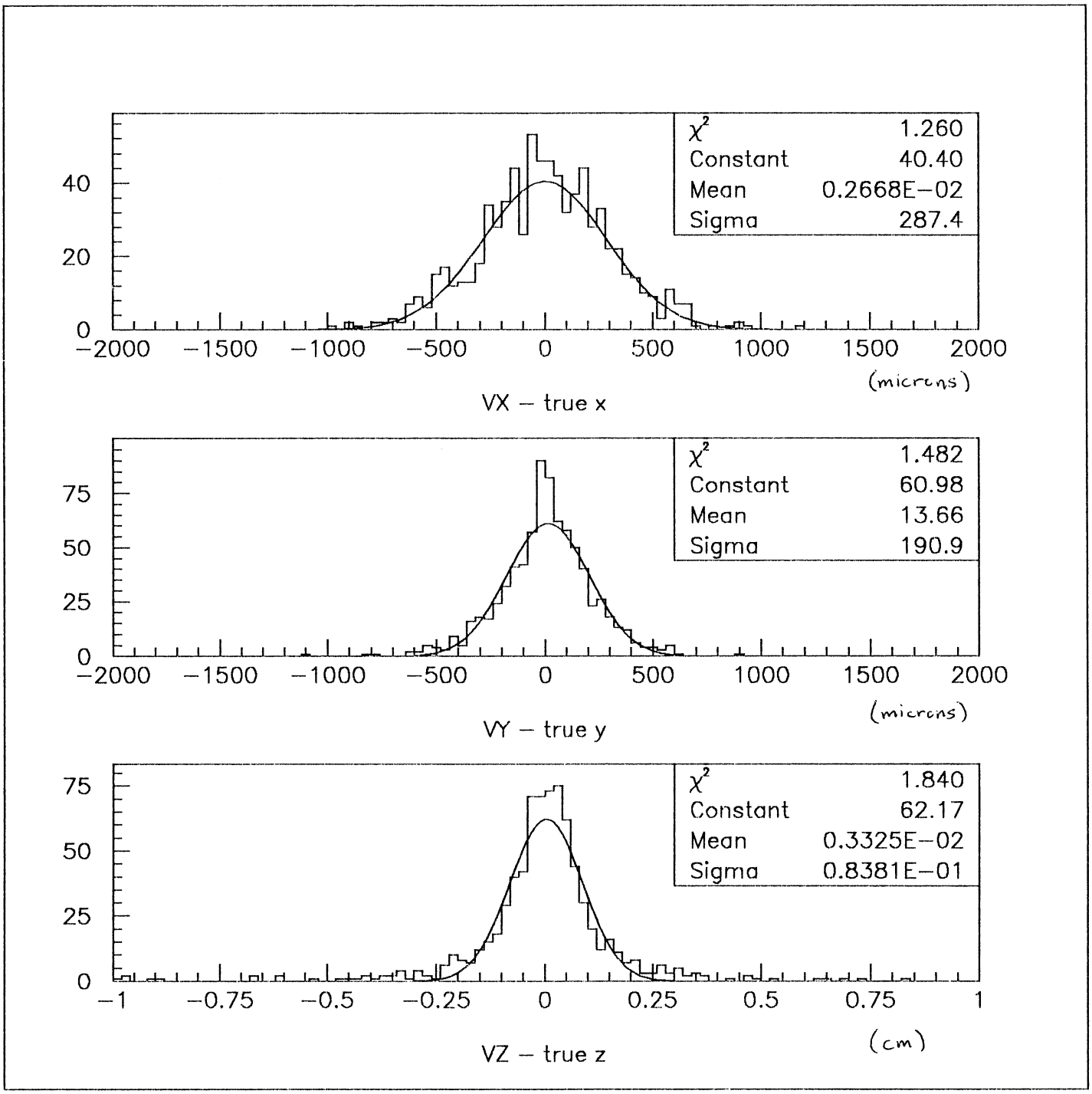
χ² 1.260
Constant 40.40
Mean 0.2668E−02
Sigma 287.4
40
20
0
−2000 −1500 −1000 −500 0 500 1000 1500 2000
(microns)
VX − true x
χ² 1.482
Constant 60.98
Mean 13.66
Sigma 190.9
75
50
25
0
−2000 −1500 −1000 −500 0 500 1000 1500 2000
(microns)
VY − true y
χ² 1.840
Constant 62.17
Mean 0.3325E−02
Sigma 0.8381E−01
75
50
25
0
−1 −0.75 −0.5 −0.25 0 0.25 0.5 0.75 1
(cm)
VZ − true z

Figure 8

Constraint Methods

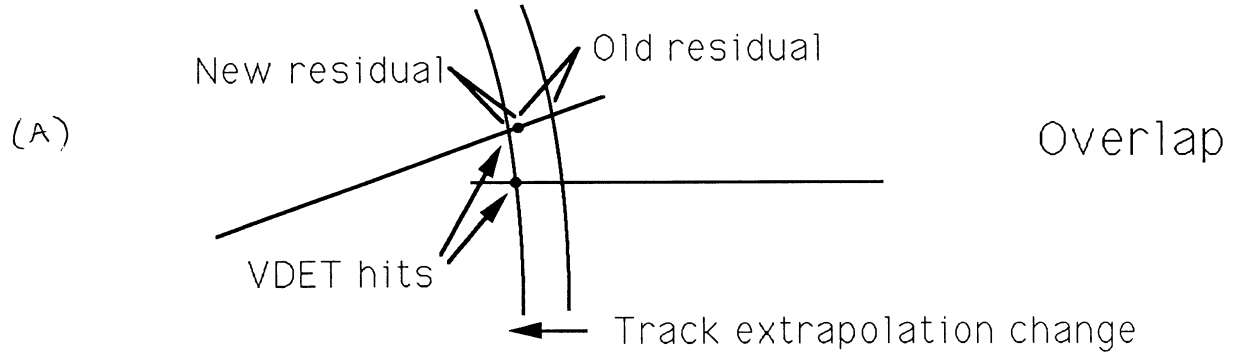

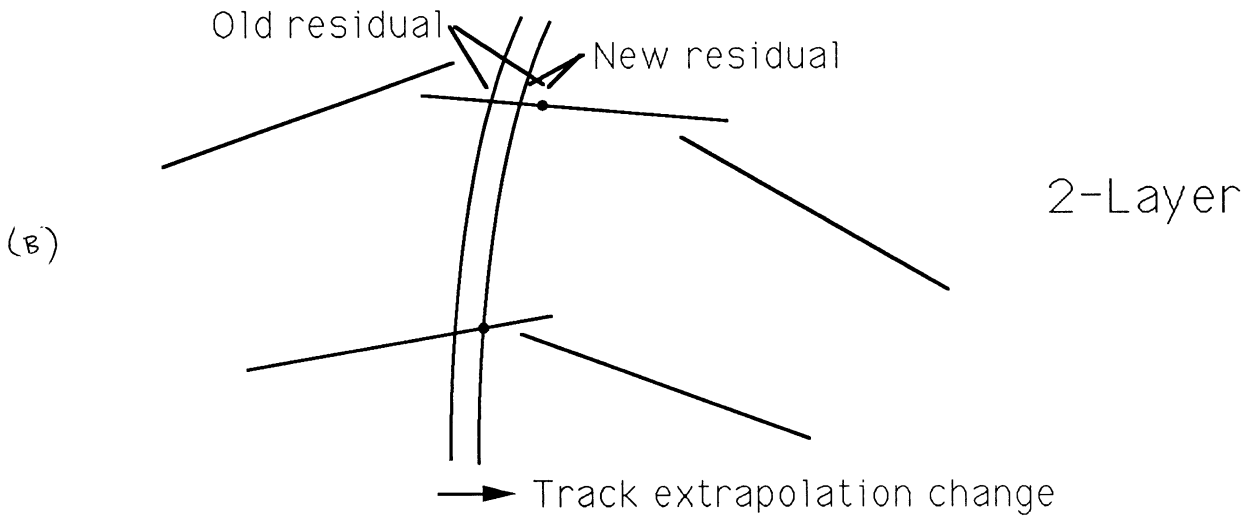

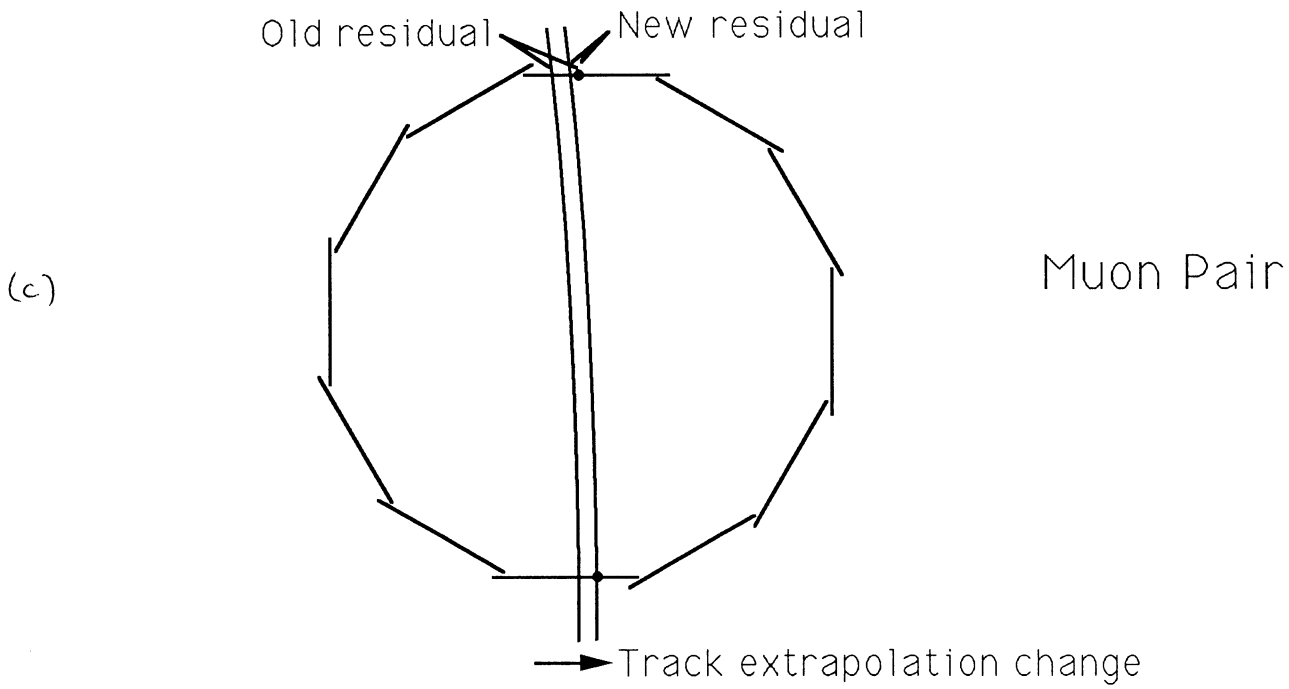

Figure 9

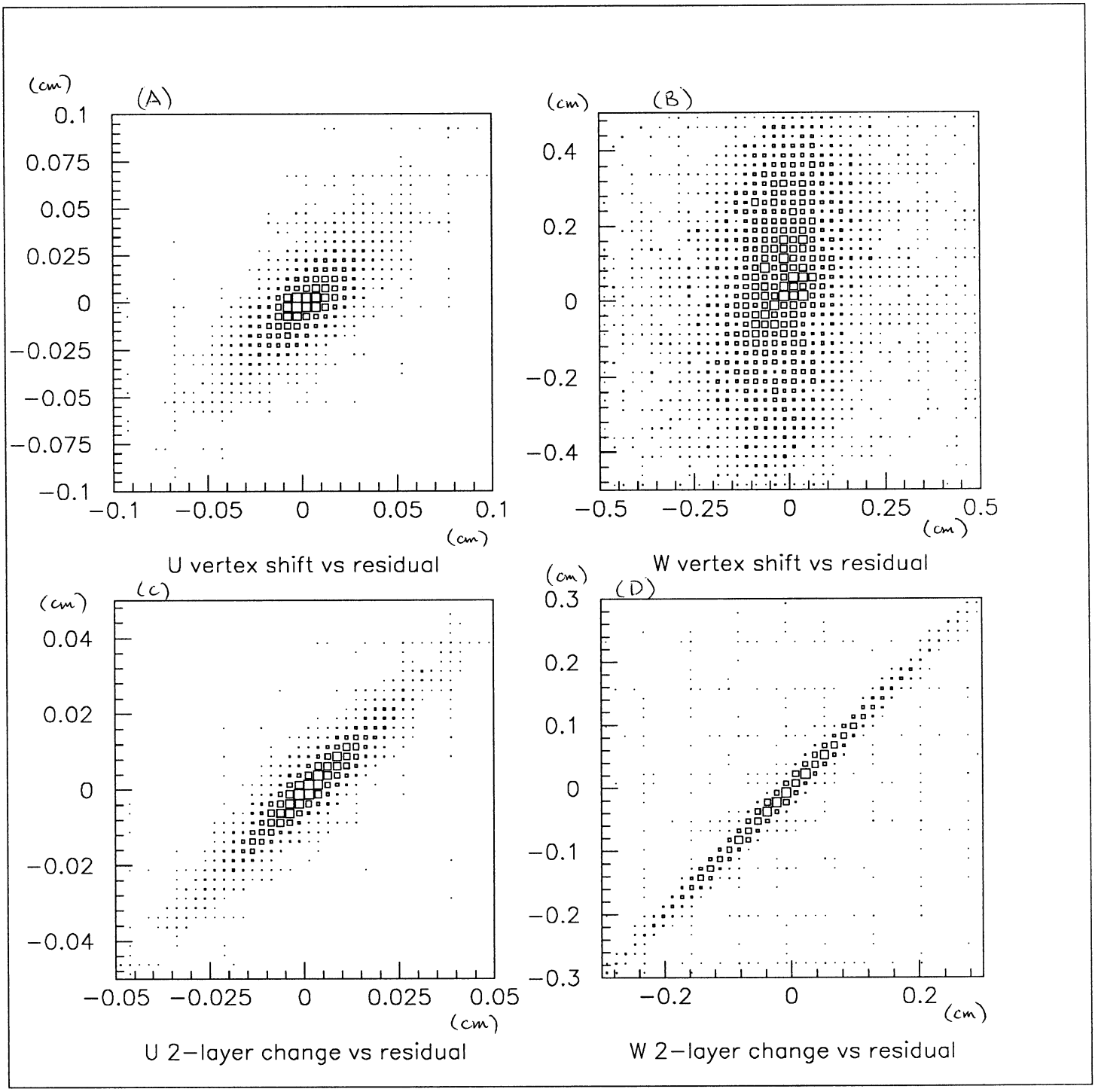
(A)
(cm)
0.1
0.075
0.05
0.025
0
−0.025
−0.05
−0.075
−0.1
−0.1
−0.05
0
0.05
0.1
(cm)
U vertex shift vs residual
(B)
(cm)
0.4
0.2
0
−0.2
−0.4
−0.5
−0.25
0
0.25
0.5
(cm)
W vertex shift vs residual
(C)
(cm)
0.04
0.02
0
−0.02
−0.04
−0.05
−0.025
0
0.025
0.05
(cm)
U 2−layer change vs residual
(D)
(cm)
0.3
0.2
0.1
0
−0.1
−0.2
−0.3
−0.2
0
0.2
(cm)
W 2−layer change vs residual

Figure 10

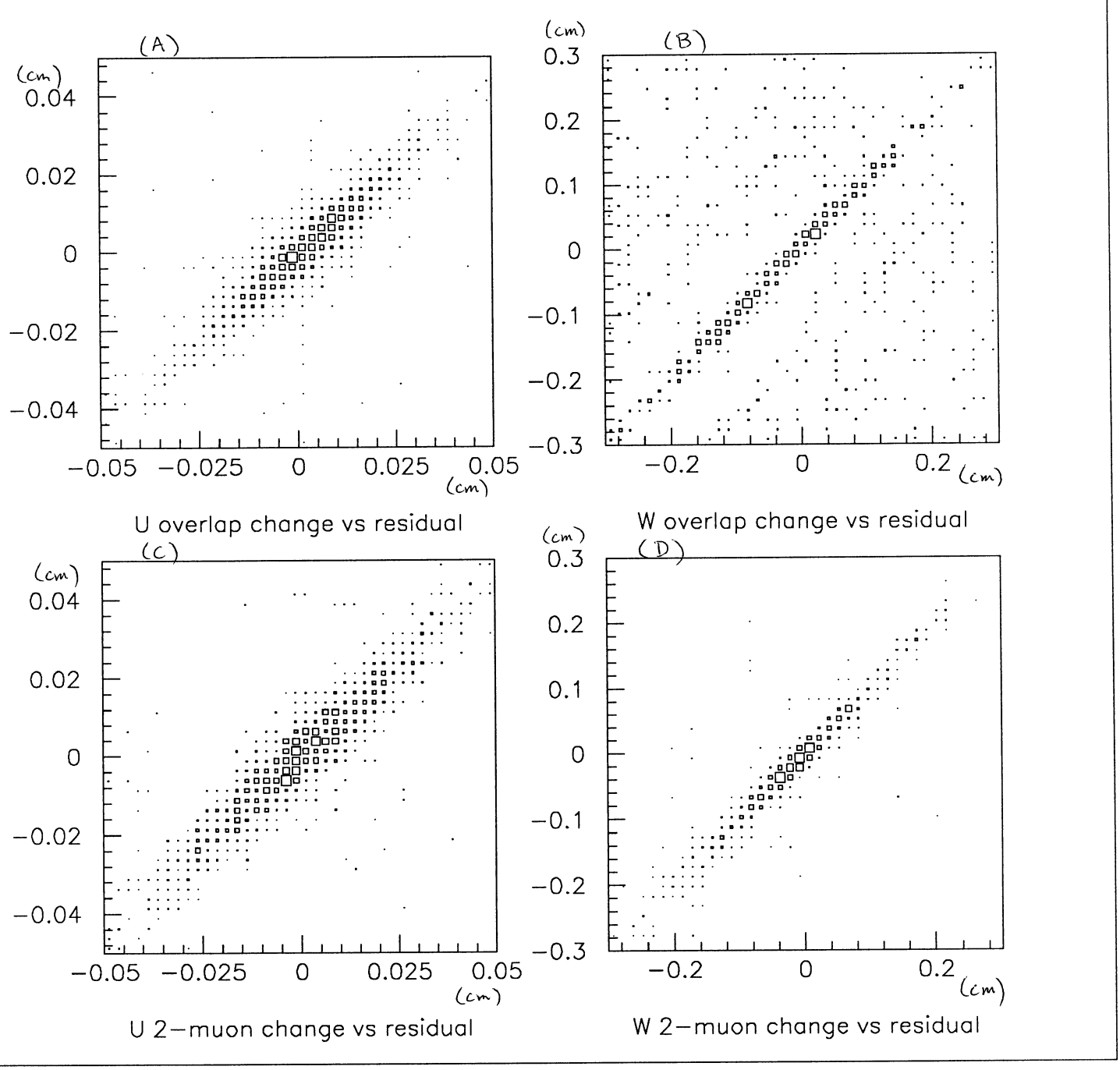
(A)
(cm)
0.04
0.02
0
−0.02
−0.04
−0.05 −0.025 0 0.025 0.05
(cm)
U overlap change vs residual
(B)
(cm)
0.3
0.2
0.1
0
−0.1
−0.2
−0.3
−0.2 0 0.2
(cm)
W overlap change vs residual
(C)
(cm)
0.04
0.02
0
−0.02
−0.04
−0.05 −0.025 0 0.025 0.05
(cm)
U 2−muon change vs residual
(D)
(cm)
0.3
0.2
0.1
0
−0.1
−0.2
−0.3
−0.2 0 0.2
(cm)
W 2−muon change vs residual

Figure 11

Global Effects of 2-layer Constraint

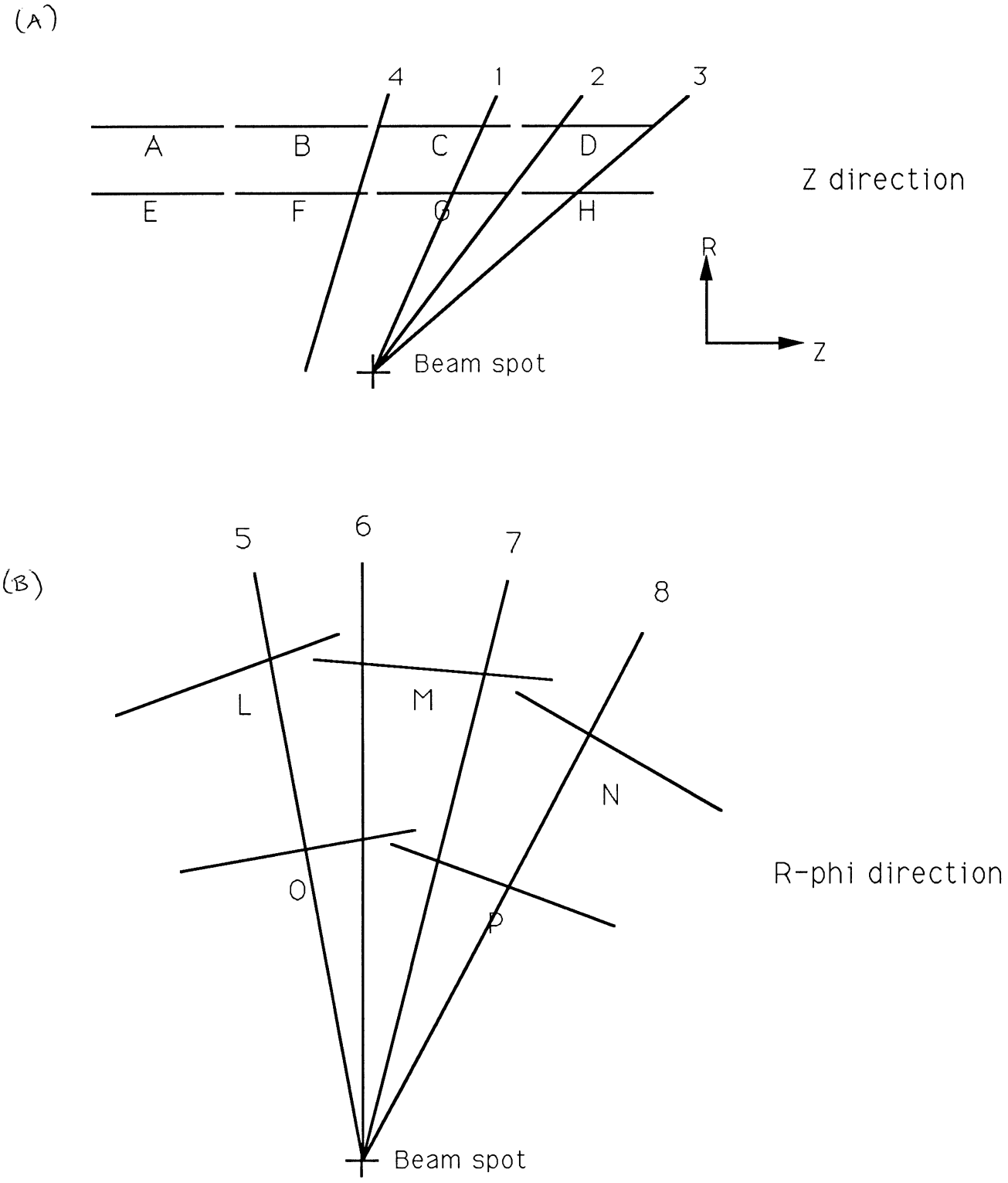

Figure 12.

VDET in 1990 ALEPH
No VDET
1 No outer layer
2 Outer layer ons OK
3 OK
4 Matching: VDPM dead
5 VDET back, OK
6 OK
7 OK
8 OK
9 OK
Fill number
Mar
Apr
May
Jun
Jul
Aug
Sep
Date
150
200
250
300
350
400

Figure 13

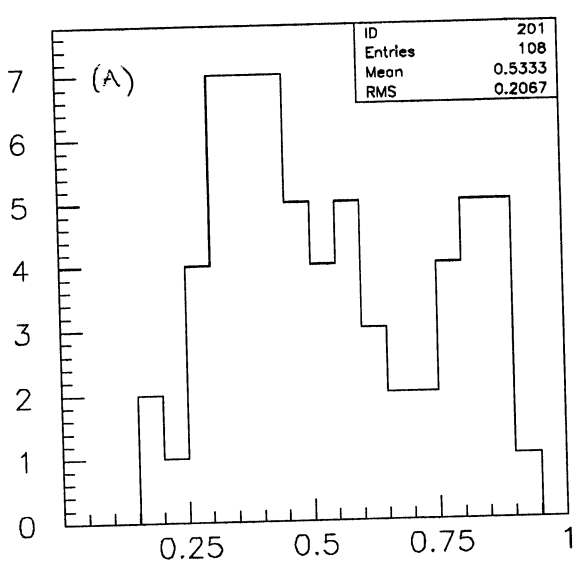

U efficiency

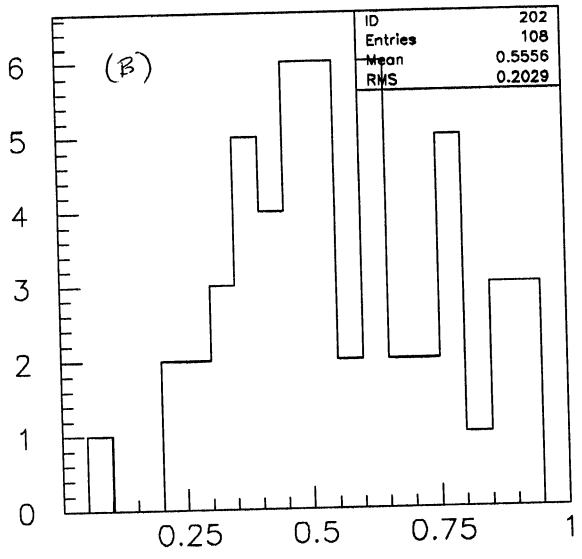

W efficiency

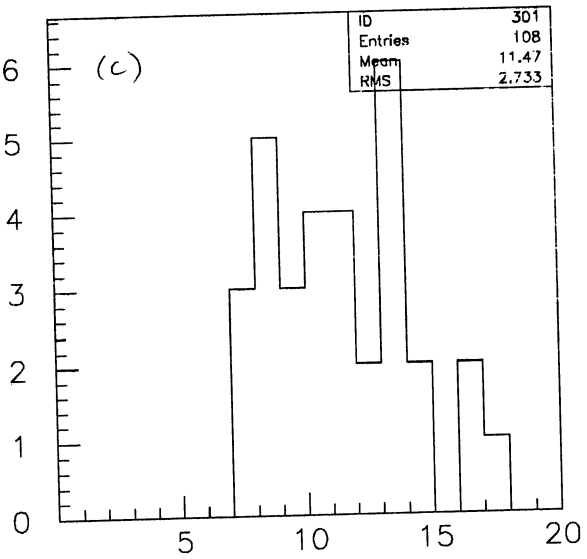

U signal/noise

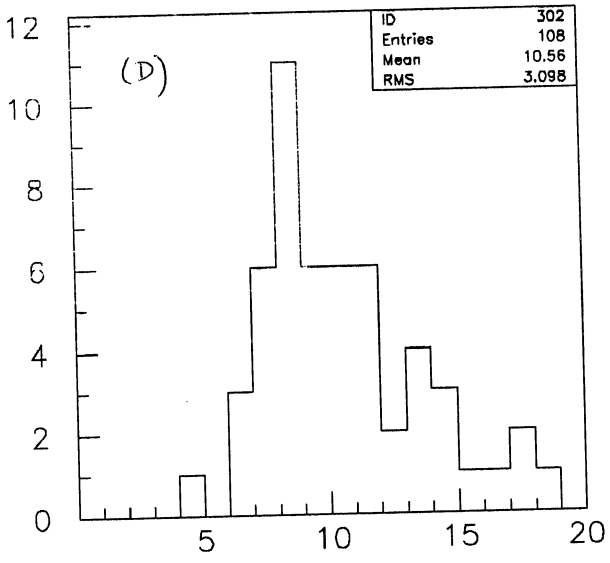

W signal/noise

Figure 14

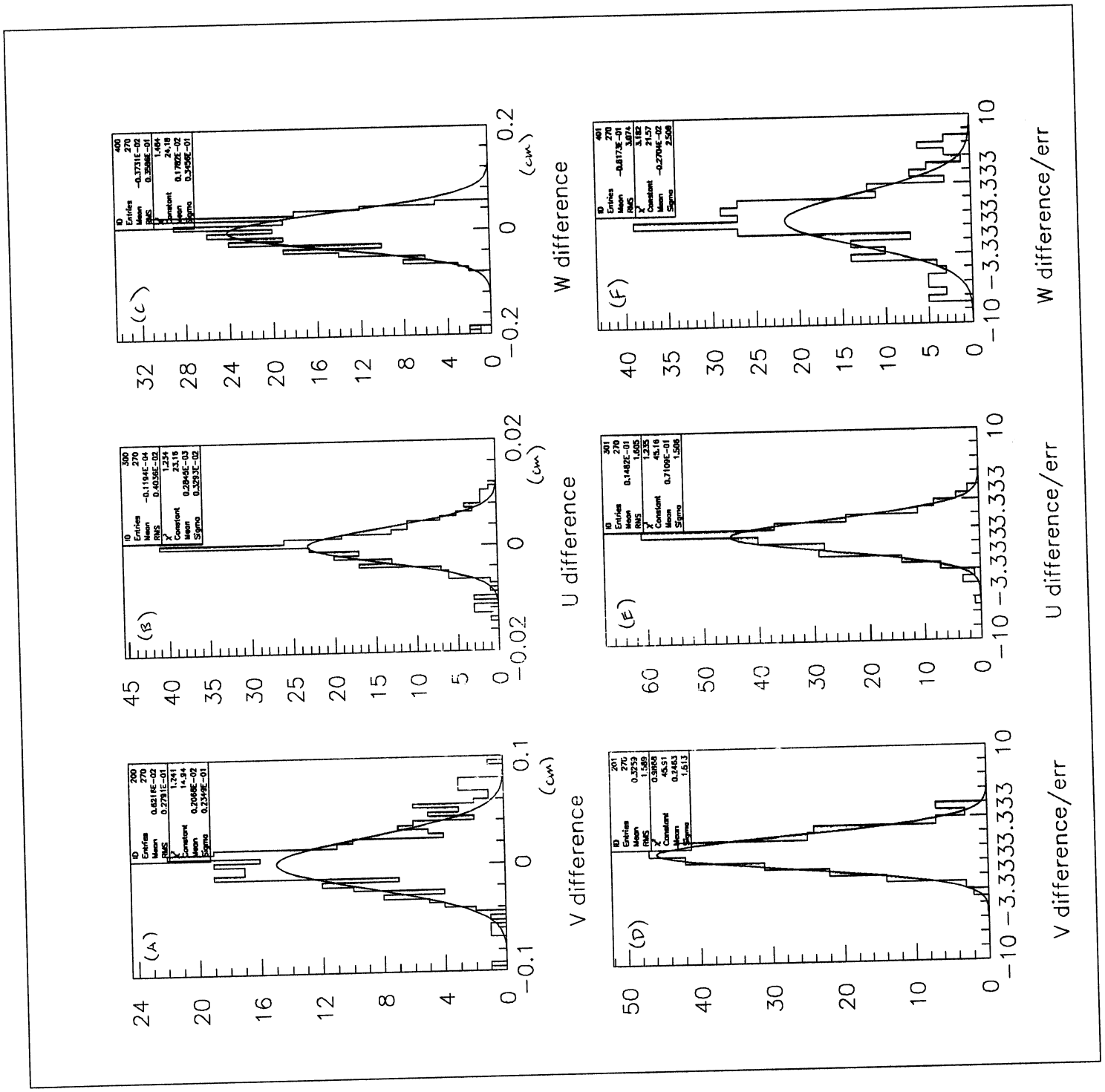
(A)
(B)
(C)
(D)
(E)
(F)
V difference
U difference
W difference
V difference/err
U difference/err
W difference/err
(cm)

Figure 15

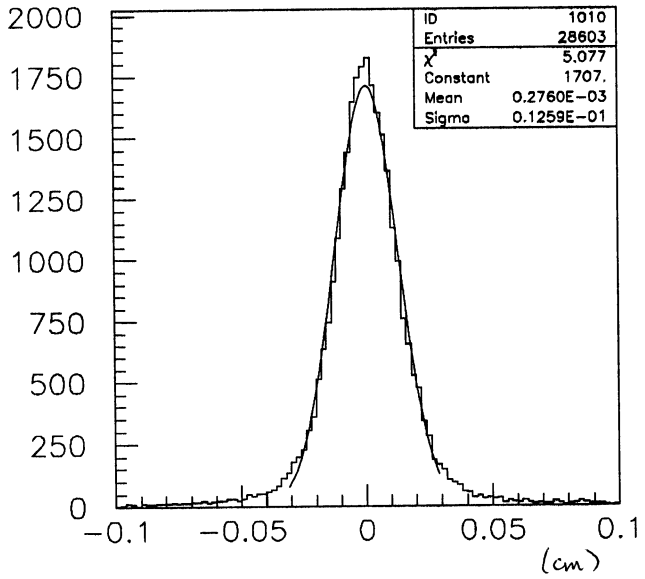

Normal U residuals

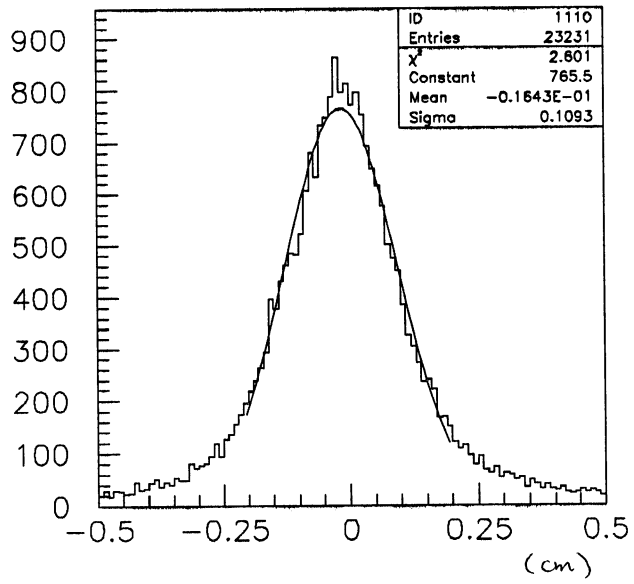

Normal W residuals

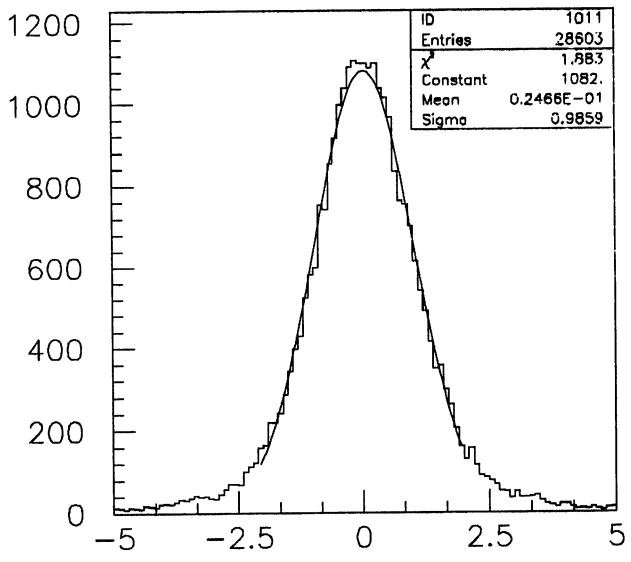

Normal U residuals/error

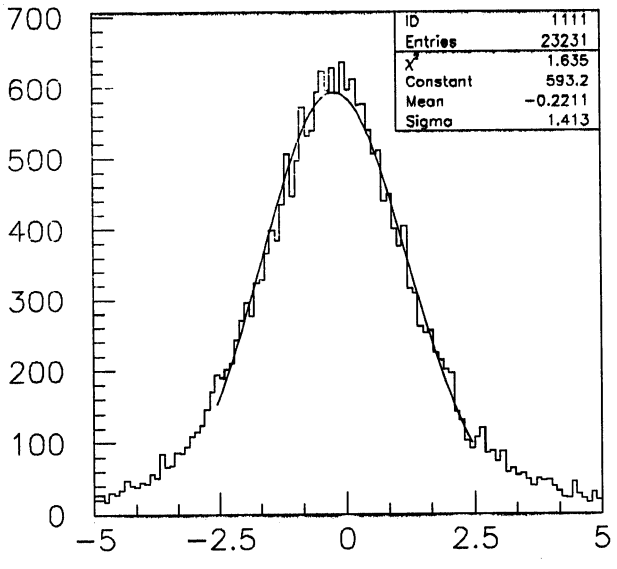

Normal W residuals/error

Figure 16.

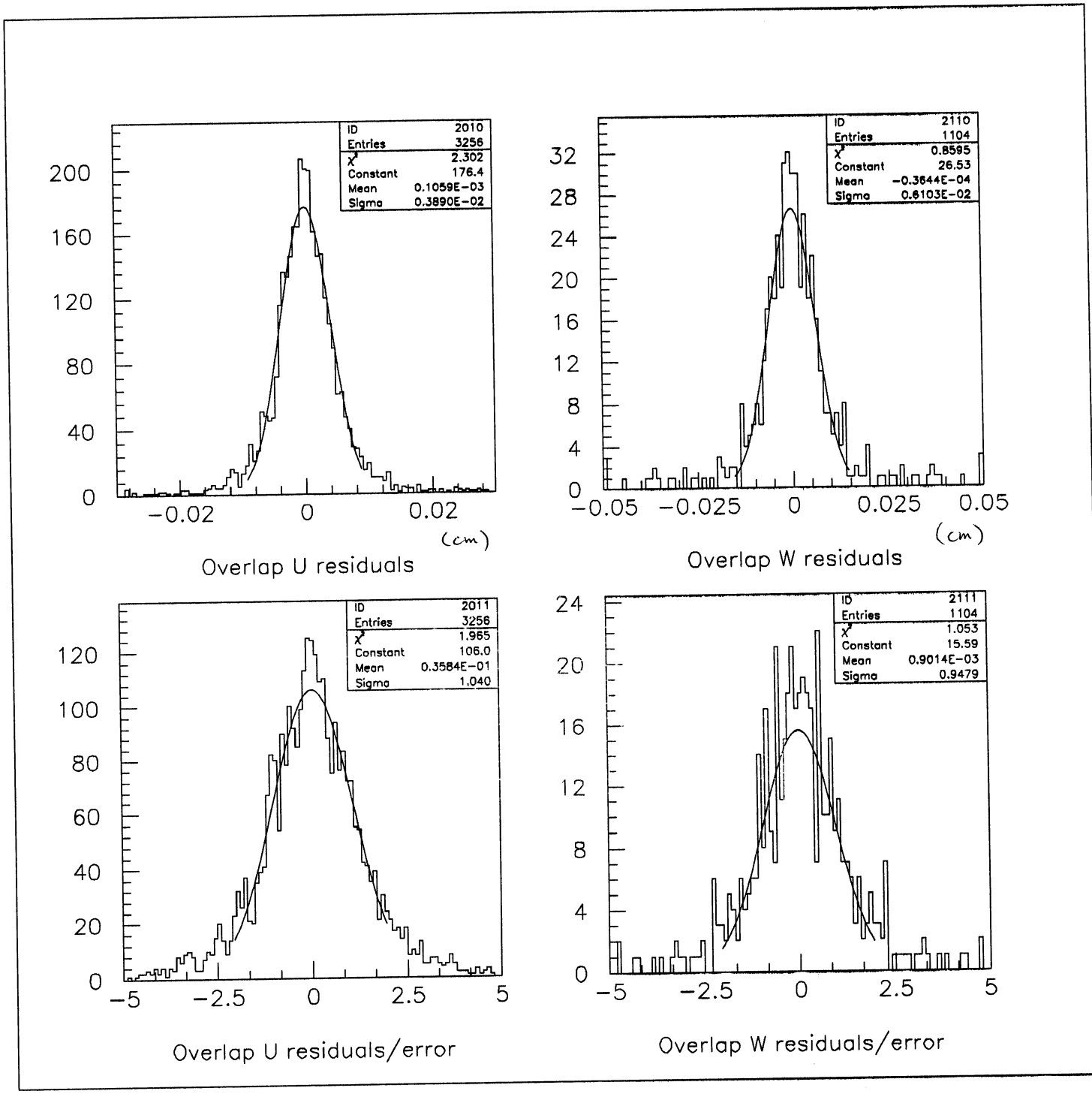
ID 2010
Entries 3256
χ² 2.302
Constant 176.4
Mean 0.1059E-03
Sigma 0.3890E-02
200
160
120
80
40
0
−0.02
0
0.02
(cm)
Overlap U residuals
ID 2110
Entries 1104
χ² 0.8595
Constant 26.53
Mean −0.3644E-04
Sigma 0.6103E-02
32
28
24
20
16
12
8
4
0
−0.05
−0.025
0
0.025
0.05
(cm)
Overlap W residuals
ID 2011
Entries 3256
χ² 1.965
Constant 106.0
Mean 0.3584E-01
Sigma 1.040
120
100
80
60
40
20
0
−5
−2.5
0
2.5
5
Overlap U residuals/error
ID 2111
Entries 1104
χ² 1.053
Constant 15.59
Mean 0.9014E-03
Sigma 0.9479
24
20
16
12
8
4
0
−5
−2.5
0
2.5
5
Overlap W residuals/error

Figure 17.

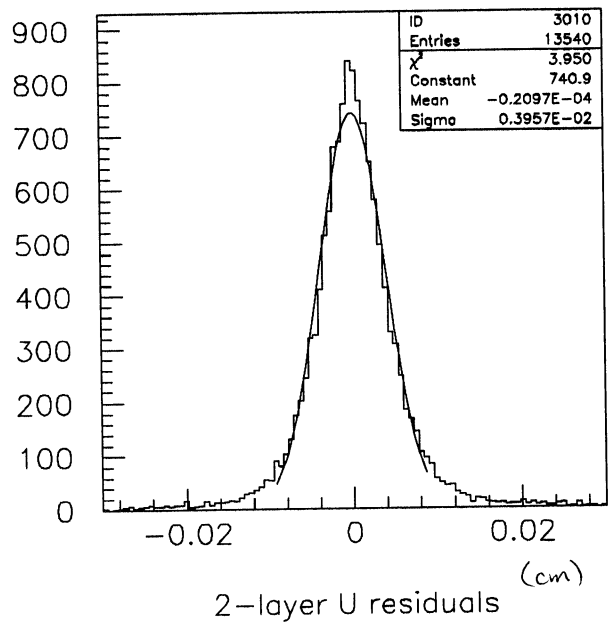

2−layer U residuals

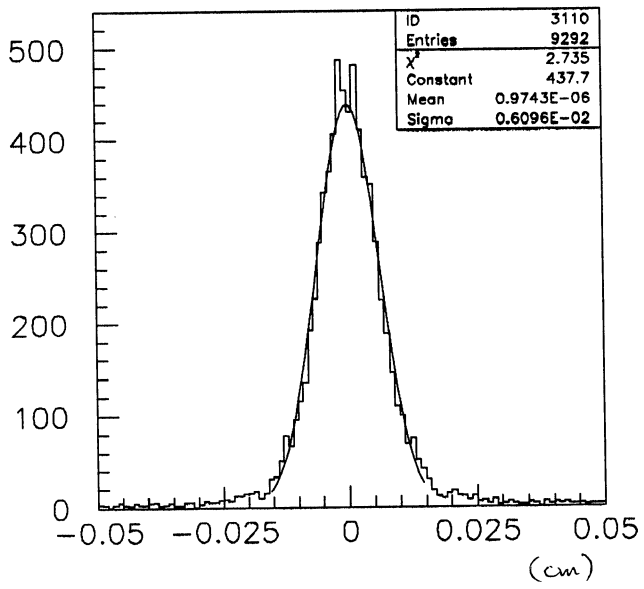

2−layer W residuals

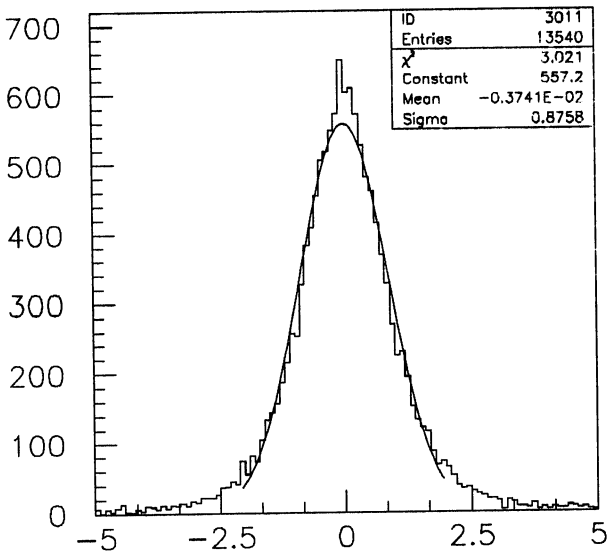

2−layer U residuals/error

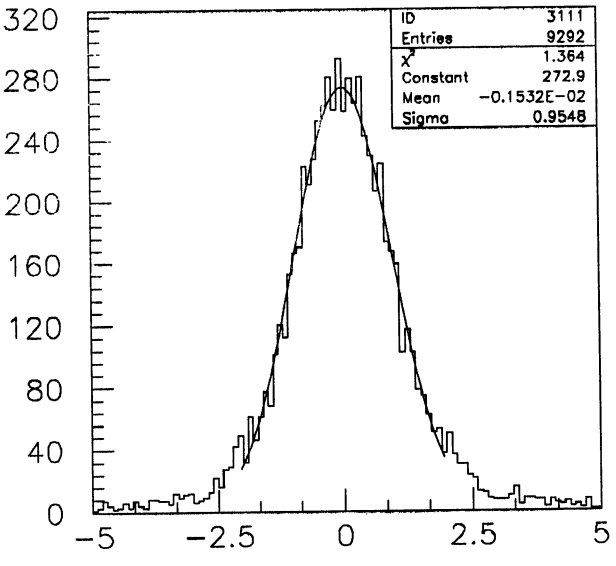

2−layer W residuals/error

Figure 18

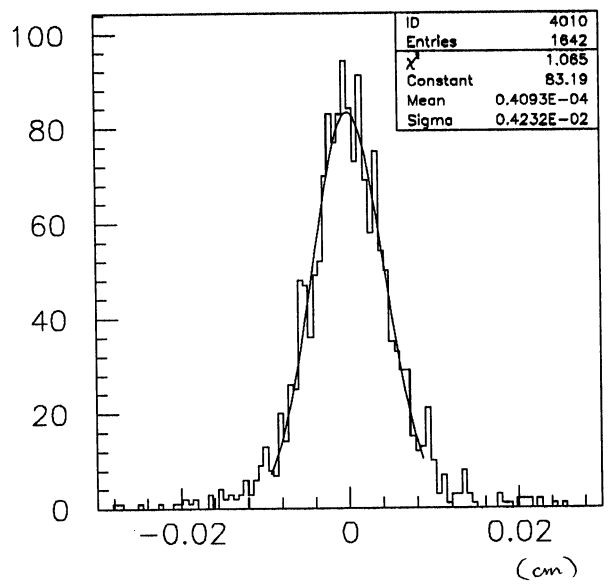

2−muon U residuals

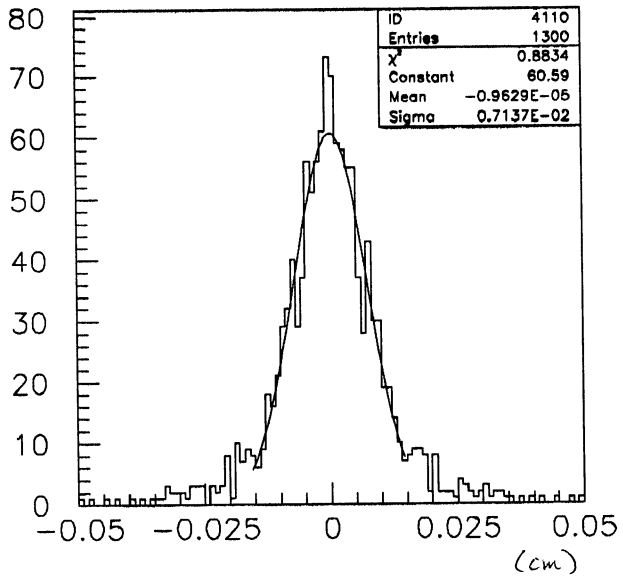

2−muon W residuals

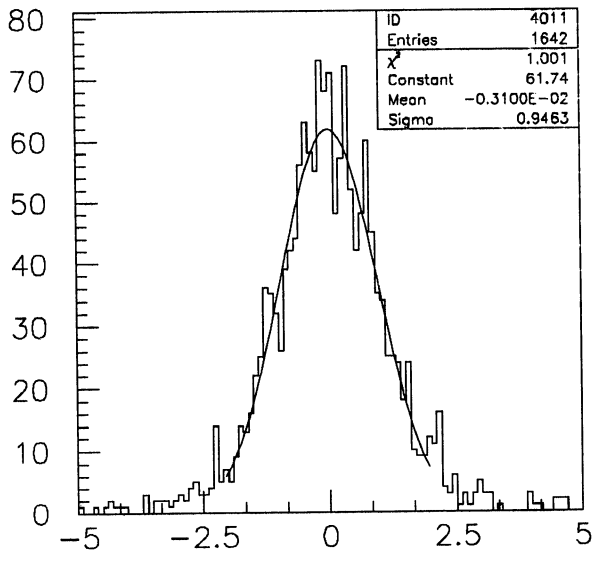

2−muon U residuals/error

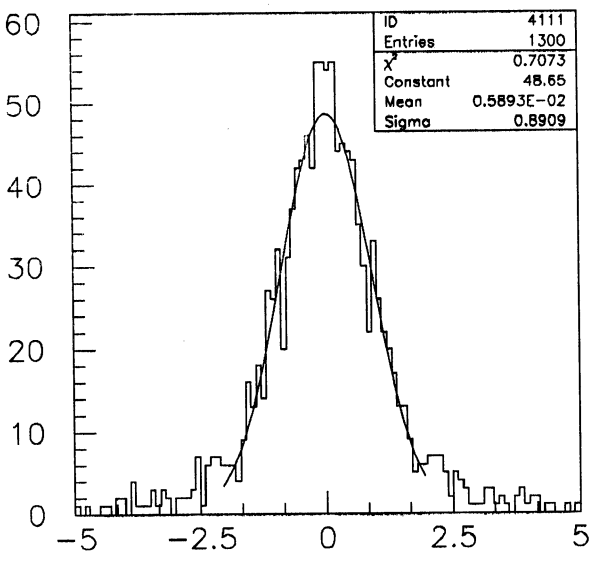

2−muon W residuals/error

Figure 19.

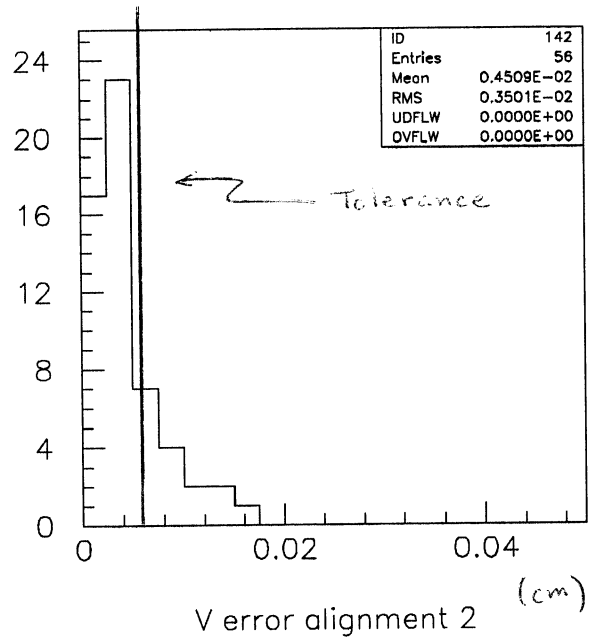

V error alignment 2

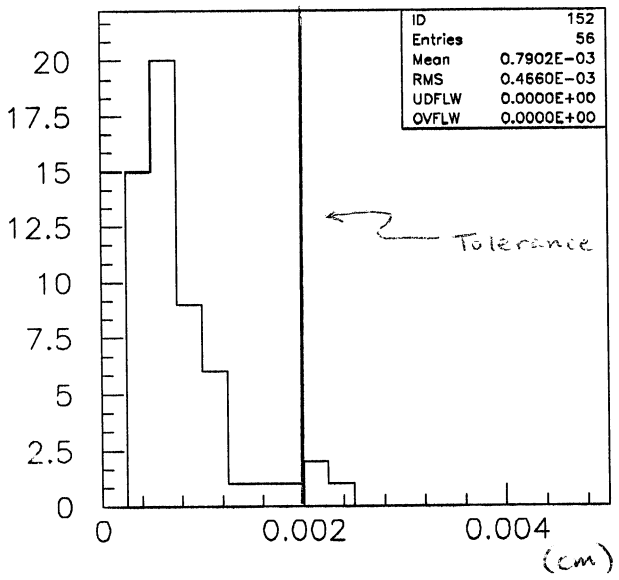

U error alignment 2

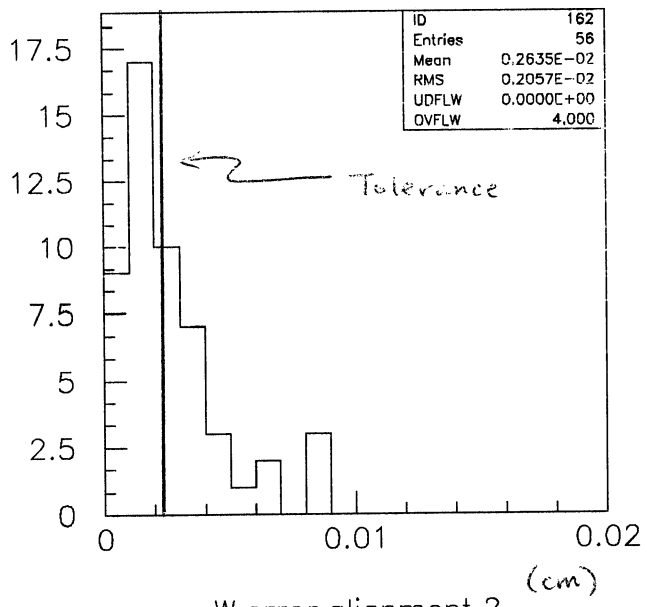

W error alignment 2

Figure 20.

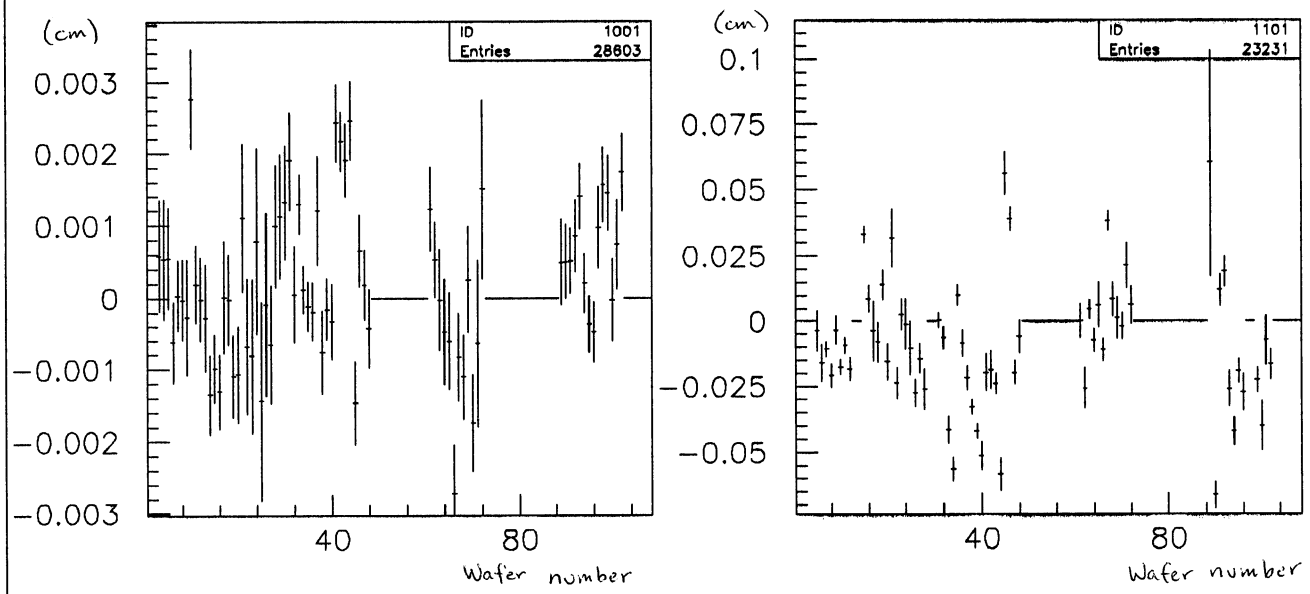

Normal U residuals by wafer

Normal W residuals by wafer

Overlap U residuals by wafer

Overlap W residuals by wafer

Figure 21

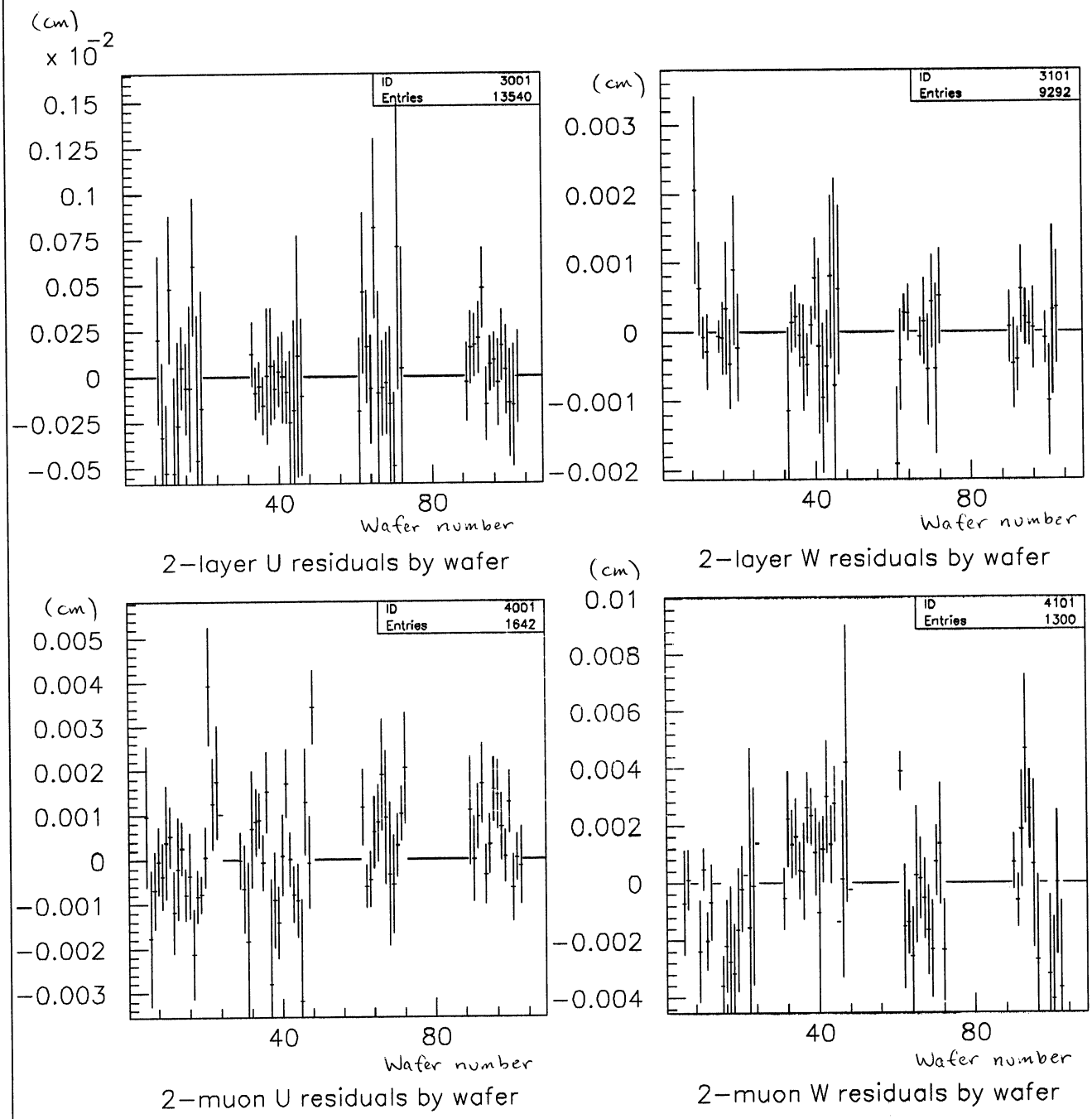
(cm)
x 10^-2
0.15
0.125
0.1
0.075
0.05
0.025
0
−0.025
−0.05
ID 3001
Entries 13540
40
80
Wafer number
2−layer U residuals by wafer
(cm)
0.003
0.002
0.001
0
−0.001
−0.002
ID 3101
Entries 9292
40
80
Wafer number
2−layer W residuals by wafer
(cm)
0.005
0.004
0.003
0.002
0.001
0
−0.001
−0.002
−0.003
ID 4001
Entries 1642
40
80
Wafer number
2−muon U residuals by wafer
(cm)
0.01
0.008
0.006
0.004
0.002
0
−0.002
−0.004
ID 4101
Entries 1300
40
80
Wafer number
2−muon W residuals by wafer

Figure 22

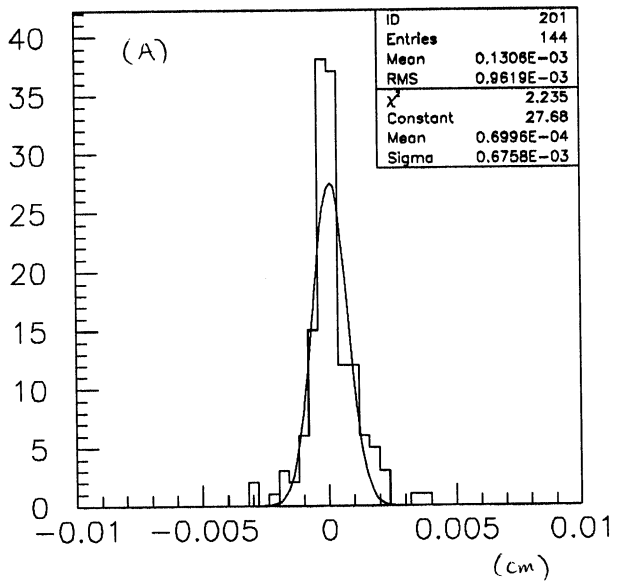

U difference

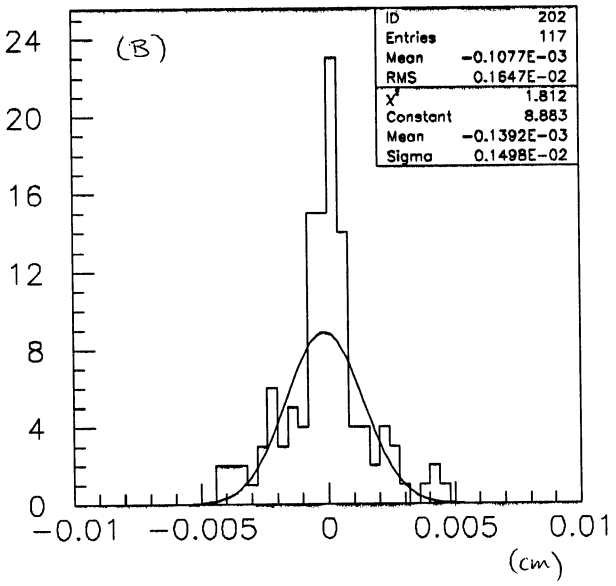

W difference

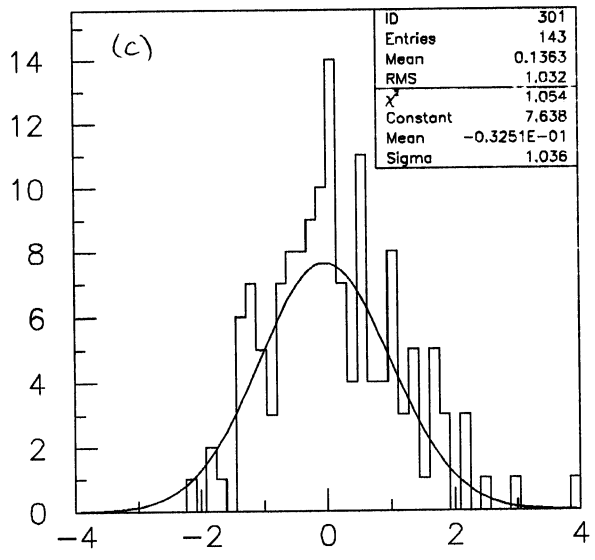

U difference/err

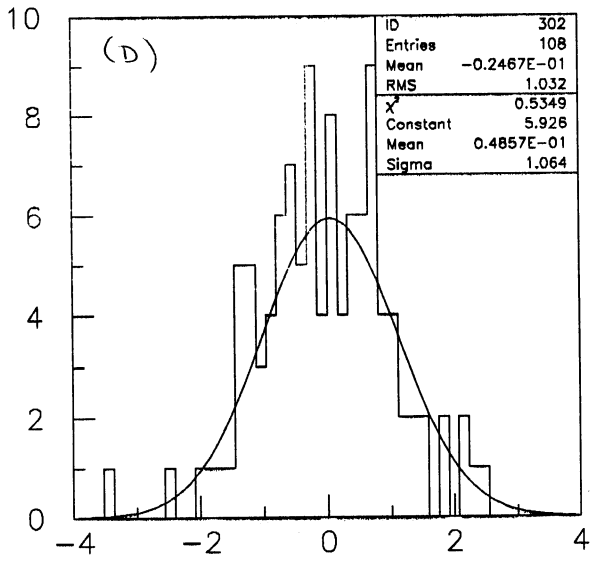

W difference/err

Figure 23.

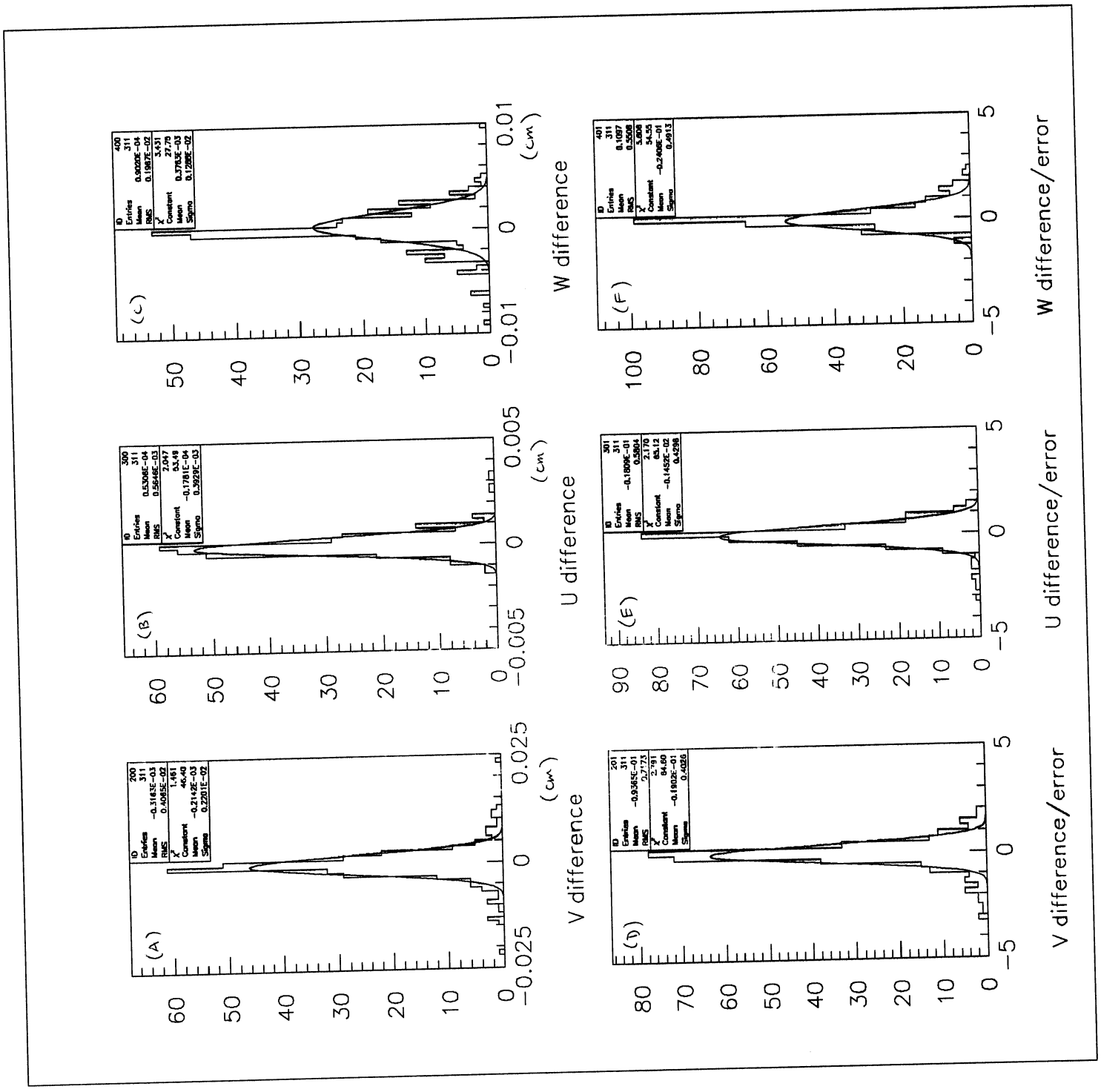
(A)
(B)
(C)
(D)
(E)
(F)
V difference
U difference
W difference
V difference/error
U difference/error
W difference/error
(cm)

Figure 24.

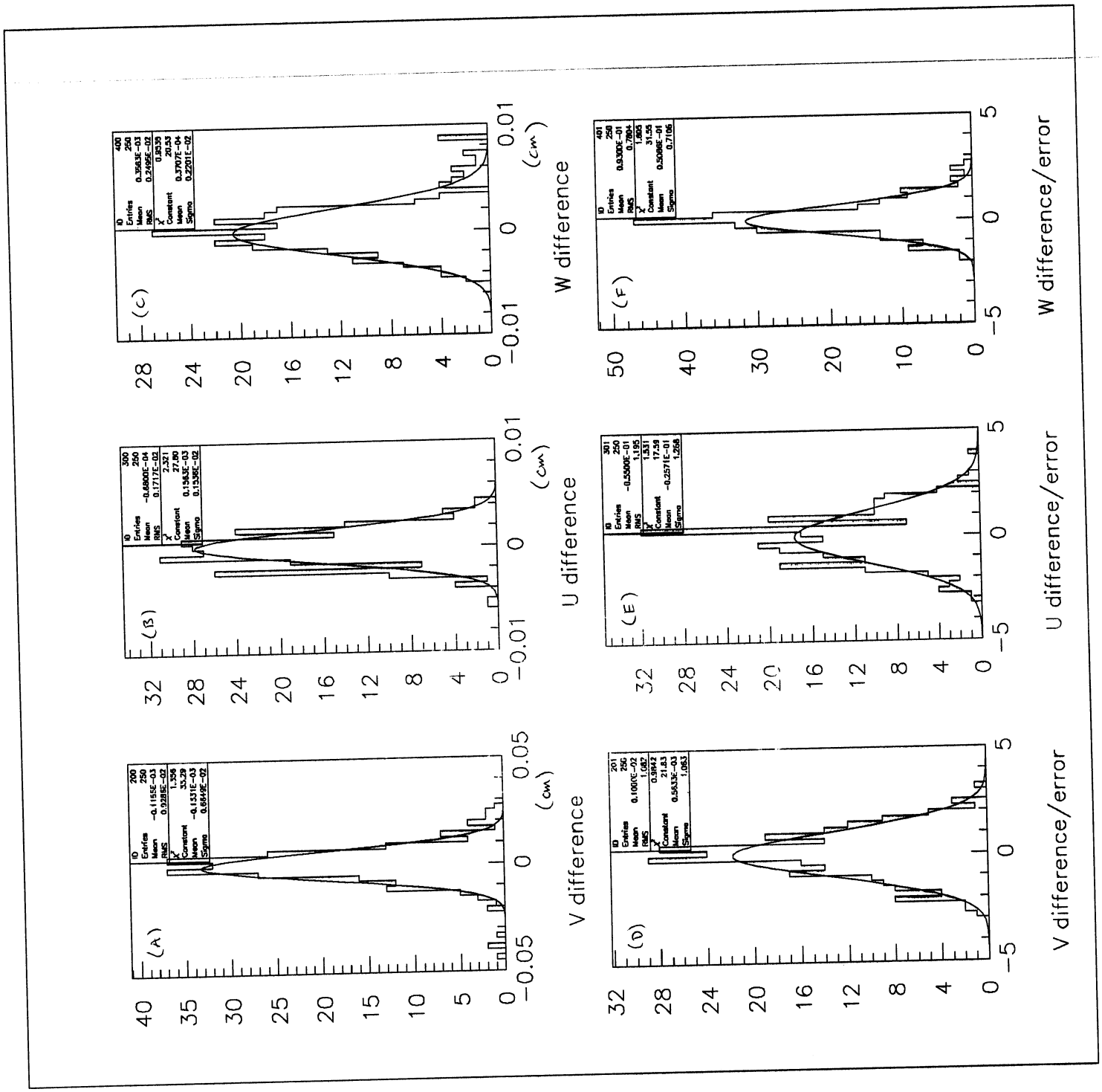
(A)
(B)
(C)
(D)
(E)
(F)
V difference
U difference
W difference
V difference/error
U difference/error
W difference/error
(cm)

Figure 25

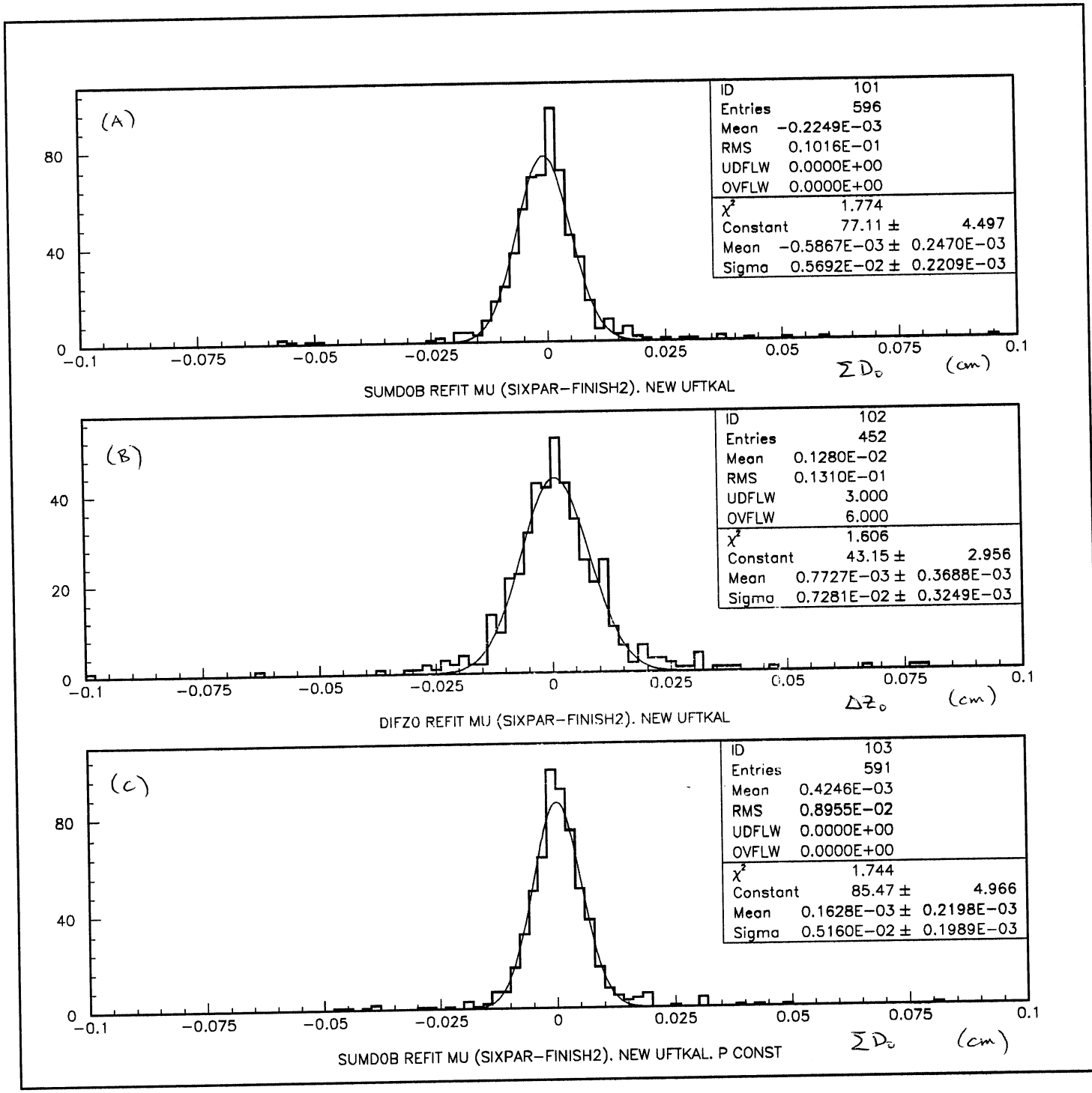
(A)
ID 101
Entries 596
Mean −0.2249E−03
RMS 0.1016E−01
UDFLW 0.0000E+00
OVFLW 0.0000E+00
χ² 1.774
Constant 77.11 ± 4.497
Mean −0.5867E−03 ± 0.2470E−03
Sigma 0.5692E−02 ± 0.2209E−03
80
40
0
−0.1
−0.075
−0.05
−0.025
0
0.025
0.05
0.075
0.1
ΣD₀ (cm)
SUMD0B REFIT MU (SIXPAR−FINISH2). NEW UFTKAL
(B)
ID 102
Entries 452
Mean 0.1280E−02
RMS 0.1310E−01
UDFLW 3.000
OVFLW 6.000
χ² 1.606
Constant 43.15 ± 2.956
Mean 0.7727E−03 ± 0.3688E−03
Sigma 0.7281E−02 ± 0.3249E−03
40
20
0
−0.1
−0.075
−0.05
−0.025
0
0.025
0.05
0.075
0.1
ΔZ₀ (cm)
DIFZ0 REFIT MU (SIXPAR−FINISH2). NEW UFTKAL
(C)
ID 103
Entries 591
Mean 0.4246E−03
RMS 0.8955E−02
UDFLW 0.0000E+00
OVFLW 0.0000E+00
χ² 1.744
Constant 85.47 ± 4.966
Mean 0.1628E−03 ± 0.2198E−03
Sigma 0.5160E−02 ± 0.1989E−03
80
40
0
−0.1
−0.075
−0.05
−0.025
0
0.025
0.05
0.075
0.1
ΣD₀ (cm)
SUMD0B REFIT MU (SIXPAR−FINISH2). NEW UFTKAL. P CONST

Figure 26.

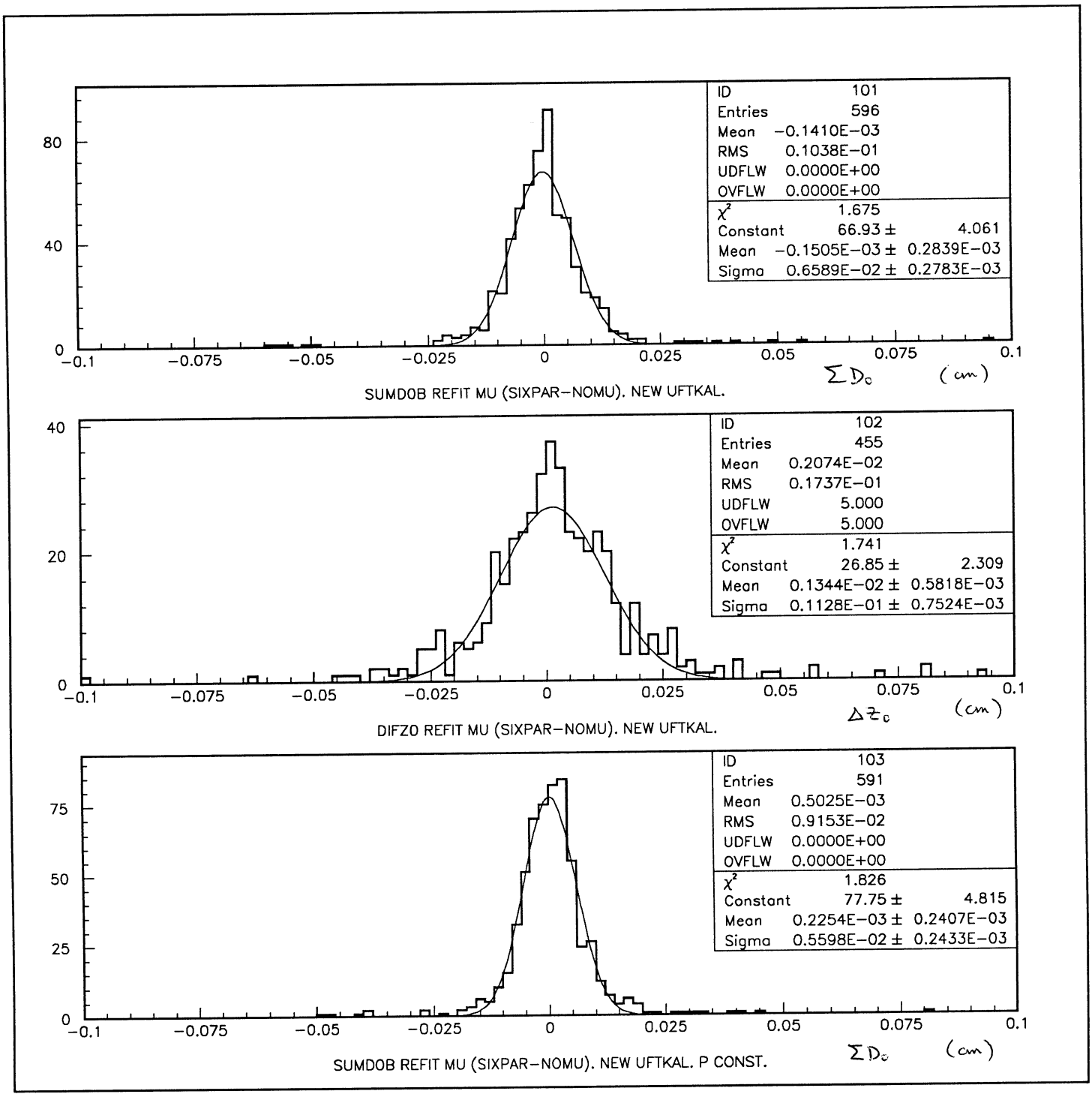
ID 101
Entries 596
Mean −0.1410E−03
RMS 0.1038E−01
UDFLW 0.0000E+00
OVFLW 0.0000E+00
χ² 1.675
Constant 66.93 ± 4.061
Mean −0.1505E−03 ± 0.2839E−03
Sigma 0.6589E−02 ± 0.2783E−03
ΣD₀ (cm)
SUMDOB REFIT MU (SIXPAR−NOMU). NEW UFTKAL.
ID 102
Entries 455
Mean 0.2074E−02
RMS 0.1737E−01
UDFLW 5.000
OVFLW 5.000
χ² 1.741
Constant 26.85 ± 2.309
Mean 0.1344E−02 ± 0.5818E−03
Sigma 0.1128E−01 ± 0.7524E−03
ΔZ₀ (cm)
DIFZO REFIT MU (SIXPAR−NOMU). NEW UFTKAL.
ID 103
Entries 591
Mean 0.5025E−03
RMS 0.9153E−02
UDFLW 0.0000E+00
OVFLW 0.0000E+00
χ² 1.826
Constant 77.75 ± 4.815
Mean 0.2254E−03 ± 0.2407E−03
Sigma 0.5598E−02 ± 0.2433E−03
ΣD₀ (cm)
SUMDOB REFIT MU (SIXPAR−NOMU). NEW UFTKAL. P CONST.

Figure 27.

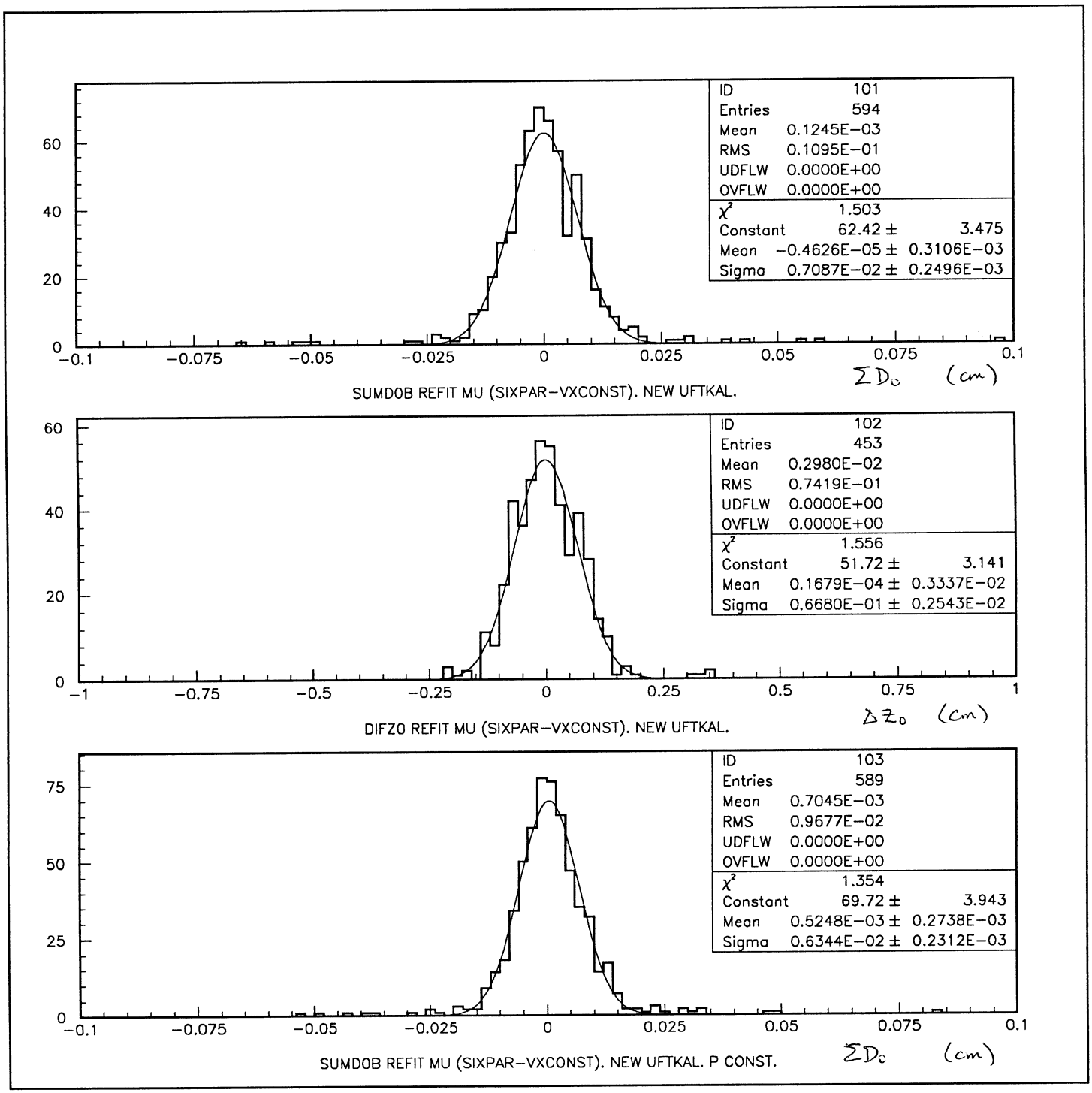
ID 101
Entries 594
Mean 0.1245E−03
RMS 0.1095E−01
UDFLW 0.0000E+00
OVFLW 0.0000E+00
χ² 1.503
Constant 62.42 ± 3.475
Mean −0.4626E−05 ± 0.3106E−03
Sigma 0.7087E−02 ± 0.2496E−03
ΣD₀ (cm)
SUMD0B REFIT MU (SIXPAR−VXCONST). NEW UFTKAL.
ID 102
Entries 453
Mean 0.2980E−02
RMS 0.7419E−01
UDFLW 0.0000E+00
OVFLW 0.0000E+00
χ² 1.556
Constant 51.72 ± 3.141
Mean 0.1679E−04 ± 0.3337E−02
Sigma 0.6680E−01 ± 0.2543E−02
ΔZ₀ (cm)
DIFZ0 REFIT MU (SIXPAR−VXCONST). NEW UFTKAL.
ID 103
Entries 589
Mean 0.7045E−03
RMS 0.9677E−02
UDFLW 0.0000E+00
OVFLW 0.0000E+00
χ² 1.354
Constant 69.72 ± 3.943
Mean 0.5248E−03 ± 0.2738E−03
Sigma 0.6344E−02 ± 0.2312E−03
ΣD₀ (cm)
SUMD0B REFIT MU (SIXPAR−VXCONST). NEW UFTKAL. P CONST.

Figure 28

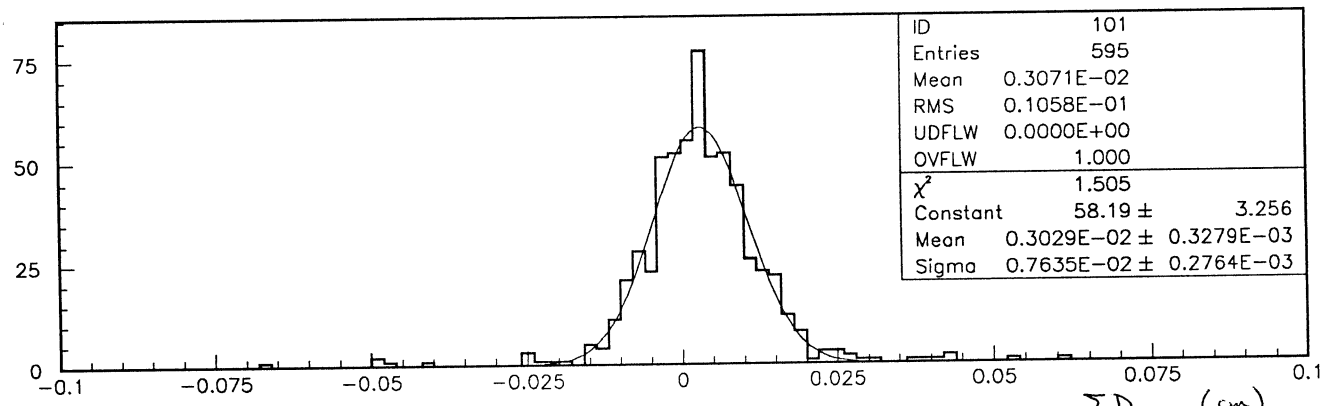

SUMDOB REFIT MU (SIXPAR−NOCONST3). NEW UFTKAL.

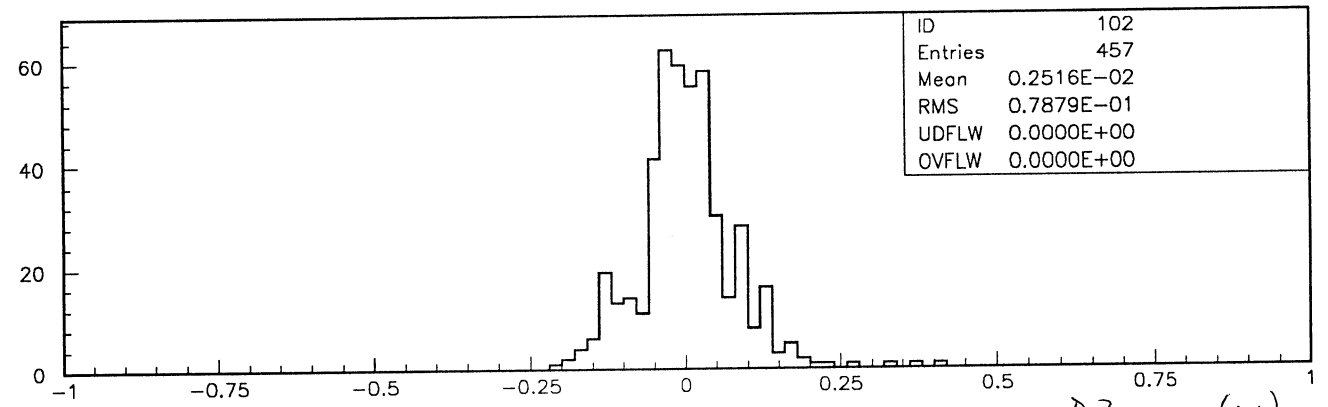

DIFZO REFIT MU (SIXPAR−NOCONST3). NEW UFTKAL.

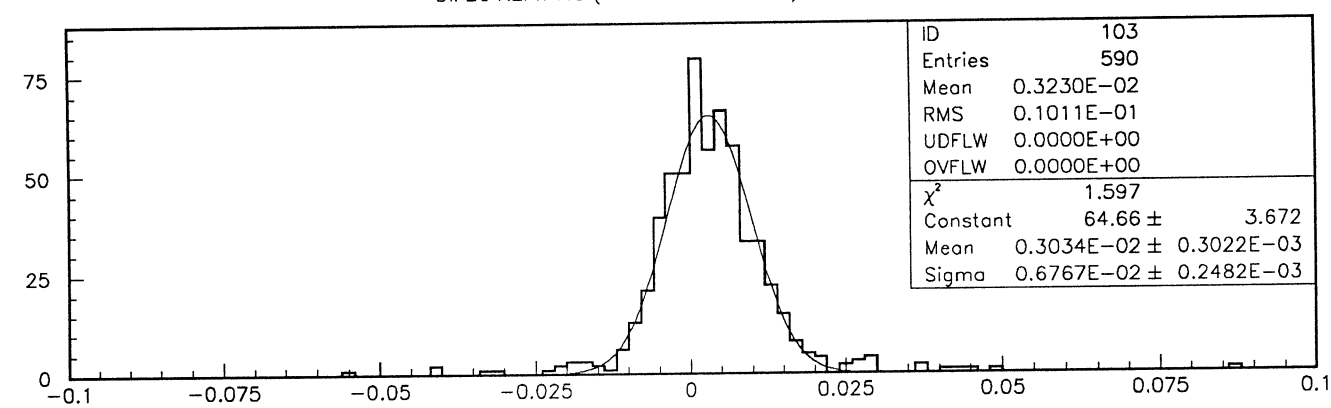

SUMDOB REFIT MU (SIXPAR−NOCONST3). NEW UFTKAL. P CONST.

Figure 29.

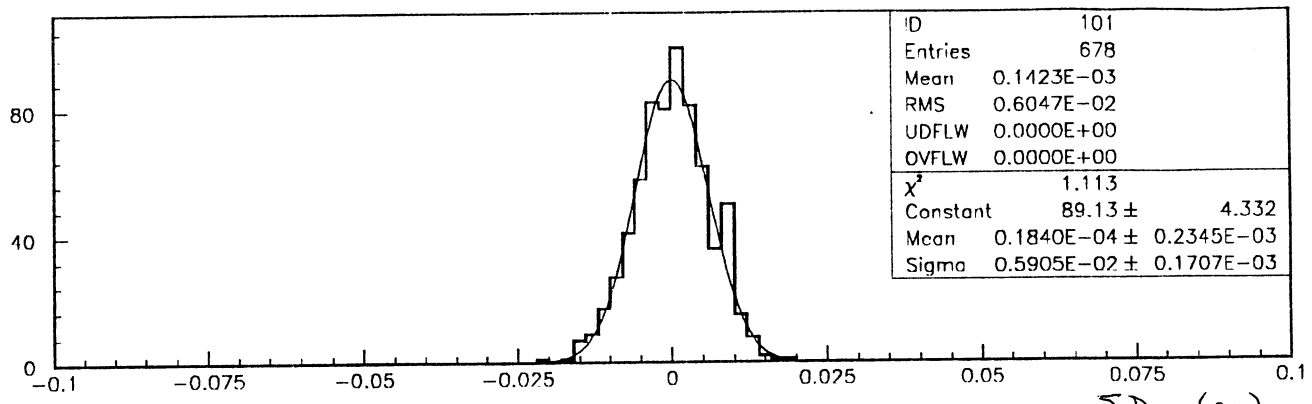

SUMDO REFIT MC MUONS. 1 U HIT EACH. SIGMAU=28.3

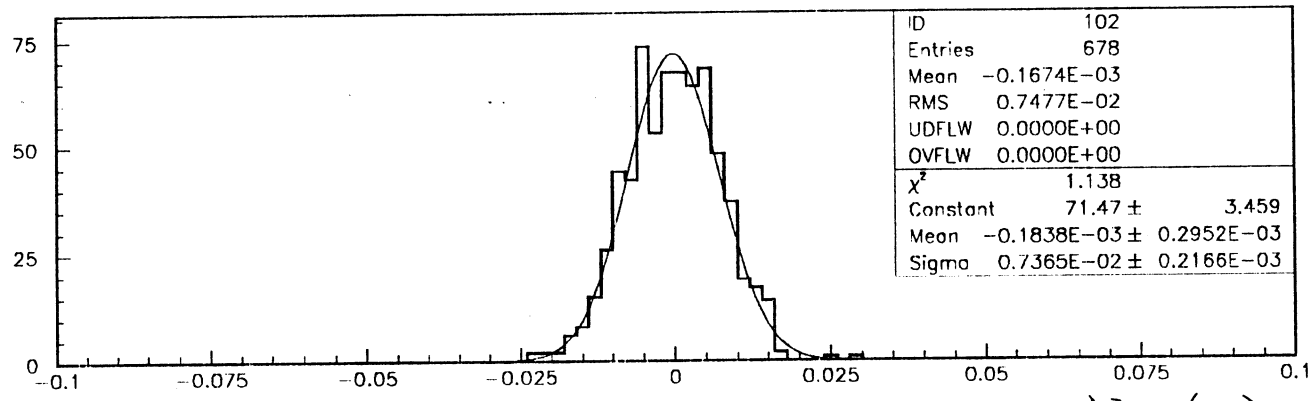

DIFZ0 REFIT MC MUONS. 1 W HIT EACH. SIGMAW=42.4

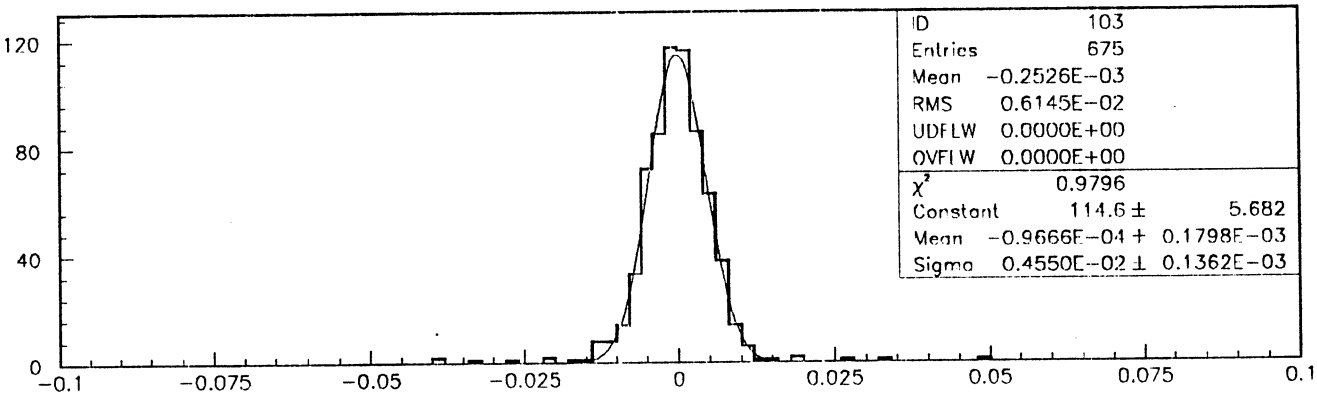

SUMDO REFIT MC MUONS. 1 U HIT EACH. SIGMAU=28.3. P CONST.

Figure 30.

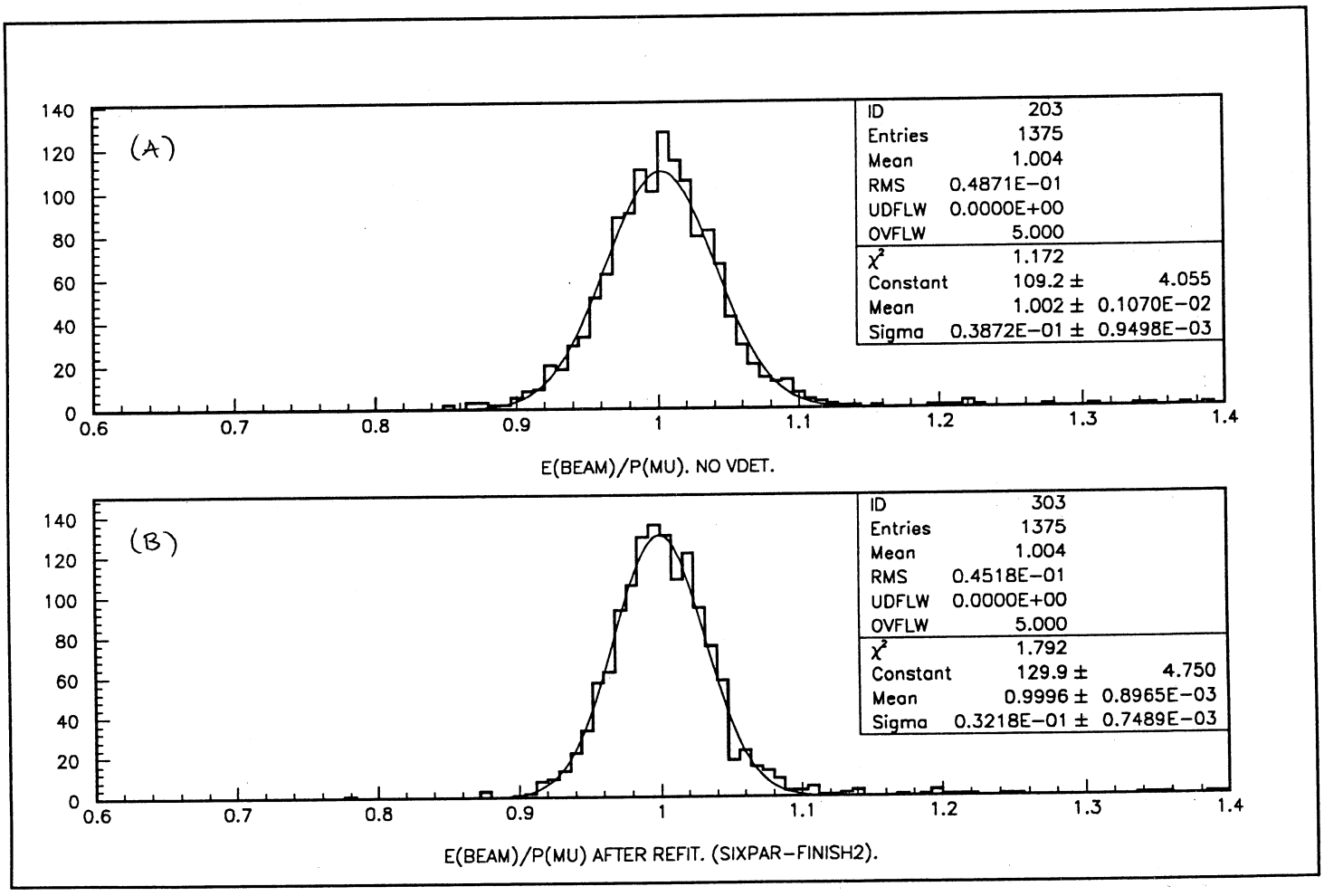
(A)
ID 203
Entries 1375
Mean 1.004
RMS 0.4871E-01
UDFLW 0.0000E+00
OVFLW 5.000
χ² 1.172
Constant 109.2 ± 4.055
Mean 1.002 ± 0.1070E-02
Sigma 0.3872E-01 ± 0.9498E-03
E(BEAM)/P(MU). NO VDET.
(B)
ID 303
Entries 1375
Mean 1.004
RMS 0.4518E-01
UDFLW 0.0000E+00
OVFLW 5.000
χ² 1.792
Constant 129.9 ± 4.750
Mean 0.9996 ± 0.8965E-03
Sigma 0.3218E-01 ± 0.7489E-03
E(BEAM)/P(MU) AFTER REFIT. (SIXPAR-FINISH2).